

OCTOBER 13, 1972

MDC-G3799

N73-11893

CR-128630

# CASE FILE COPY

## ADVANCED ETC/LSS COMPUTERIZED ANALYTICAL MODELS - CO<sub>2</sub> CONCENTRATION FINAL REPORT

VOLUME I   Summary Document

MCDONNELL DOUGLAS ASTRONAUTICS COMPANY

MCDONNELL DOUGLAS   
CORPORATION



ADVANCED ETC/LSS COMPUTERIZED  
ANALYTICAL MODELS - CO<sub>2</sub> CONCENTRATION  
FINAL REPORT

VOLUME I  
Summary Document

OCTOBER 13, 1972

MDC-G3799

PREPARED BY:

B. N. TAYLOR and A. V. LOSCUTOFF

APPROVED BY:

*Terence Deacon*  
60 K. H. HOUGHTON, M.D.  
CHIEF ADVANCE TECHNOLOGY ENGINEER  
BIOTECHNOLOGY AND POWER

PREPARED FOR NATIONAL AERONAUTICS AND SPACE ADMINISTRATION,  
MANNED SPACECRAFT CENTER, HOUSTON, TEXAS UNDER CONTRACT NO.  
NAS9-12076

**MCDONNELL DOUGLAS ASTRONAUTICS COMPANY-WEST**

5301 Bolsa Avenue, Huntington Beach, CA 92647

## FOREWORD

The study described in this report was prepared by the Biotechnology and Power Department of the Advance Systems and Technology Directorate, McDonnell Douglas Astronautics Company - Western Division, Huntington Beach, California. J. R. Jaax, Crew Systems Division, National Aeronautics and Space Administration, Manned Spacecraft Center (MSC) was the contract technical monitor. B. N. Taylor was the principal investigator for McDonnell Douglas. A. V. Loscutoff assisted in the preparation of the computer subroutines and simulation models. Volume I of this report is a summary of the work performed. Volume II contains detailed information concerning the preparation and usage of the analytical models.

## TABLE OF CONTENTS

	<u>Page</u>
LIST OF FIGURES . . . . .	vii
SUMMARY . . . . .	ix
SECTION 1.0 INTRODUCTION . . . . .	1
SECTION 2.0 SIMULATION MODELS FOR CO <sub>2</sub> CONCENTRATION CONCEPTS	
2.1 Steam Desorbed Resins . . . . .	5
2.2 Vacuum Desorbed Solid Amines . . . . .	13
2.3 Carbonation Cell . . . . .	18
2.4 Hydrogen Depolarized Cell . . . . .	25
2.5 Solid Electrolyte . . . . .	30
2.6 Liquid Absorption . . . . .	37
2.7 Electrodialysis . . . . .	42
2.8 Molten Carbonate . . . . .	51
2.9 Membrane Diffusion . . . . .	58
2.10 Mechanical Freezeout . . . . .	66
SECTION 3.0 CONCLUSIONS . . . . .	73
REFERENCES . . . . .	81
APPENDIX A G-189A ETC/LSS SYSTEM ANALYSIS PROGRAM DESCRIPTION	

## FIGURES

	Page
2.1-1 NASA/MDAC 90-Day Manned Test Amine Resin - CO <sub>2</sub> Concentrator System . . . . .	7
2.1-2 NASA/MDAC 90-Day Test Amine Resin CO <sub>2</sub> Concentrator Performance . . . . .	9
2.1-3 G-189A Simulation of a Typical Steam Desorbed Solid Amine CO <sub>2</sub> Concentrator . . . . .	12
2.2-1 Flow Diagram of Bench Scale Gat-0-Sorb Process . . . . .	14
2.2-2 G-189A Simulation of Vacuum Desorbed Amine Bed . . . . .	16
2.2-3 Vacuum Pump Characteristics . . . . .	17
2.3-1 Carbonation Cell CO <sub>2</sub> Collector . . . . .	19
2.3-2 Carbonation Cell Stage I - Schematic Representation . . . . .	20
2.3-3 Carbonation Cell Stage II - Schematic Representation . . . . .	21
2.3-4 G189A Carbonation Cell Connection and Definition . . . . .	24
2.4-1 Hydrogen Depolarized Cell . . . . .	26
2.4-2 HDC Schematic . . . . .	27
2.4-3 G-189A Simulation Hydrogen Depolarized Cell Concentrator . . . . .	29
2.5-1 Solid Electrolyte Cell Reactions . . . . .	31
2.5-2 Solid Electrolyte Schematic . . . . .	32
2.5-3 G189A Simulation of Solid Electrolyte Subsystem . . . . .	36
2.6-1 Liquid Absorption CO <sub>2</sub> Concentrator . . . . .	39
2.6-2 G-189A Simulation of Liquid Absorption CO <sub>2</sub> Concentrator . . . . .	41
2.7-1 Electrodialysis CO <sub>2</sub> Management System . . . . .	43
2.7-2 Electrodialysis Cell Reactions . . . . .	44
2.7-3 G-189A Simulation of Electrodialysis Concentrator . . . . .	49

## FIGURES

	Page
2.8-1 Molten Carbonate Cell . . . . .	53
2.8-2 Schematic of Cell Reactions for Molten Carbonate Cell . . .	53
2.8-3 G-189A Simulation of Molten Carbonate Concept . . . . .	56
2.9-1 Membrane Module . . . . .	59
2.9-2 Membrane Diffusion Module . . . . .	60
2.9-3 G189A Simulation of Membrane Diffusion Concept . . . . .	65
2.10-1 Mechanical Freezeout System, Non-Recoverable CO <sub>2</sub> . . . . .	67
2.10-2 Mechanical Freezeout System, Recoverable CO <sub>2</sub> . . . . .	68
2.10-3 G-189A Simulation of Mechanical Freezeout . . . . .	72

## SUMMARY

Computer simulations have been prepared for the concepts of  $\text{CO}_2$  concentration which have the potential for maintaining a  $\text{CO}_2$  partial pressure of 3.0 mmHg, or less, in a spacecraft environment. The simulations were performed using the G-189A Generalized Environmental Control computer program. In preparing the simulations, new subroutines to model the principal functional components for each concept were prepared and integrated into the existing program. Sample problems were run to demonstrate the methods of simulation and performance characteristics of the individual concepts. Comparison runs for each concept can be made for parametric values of cabin pressure, crew size, cabin air dry and wet bulb temperatures, and mission duration.

The computer simulations have pointed out that, for many of the concepts, additional laboratory testing is required to determine better data for certain subsystems parameters or physical properties. Specific recommendations for each concept are contained in section 3.0 of this report.

The analytical models provide a means of determining subsystem performance for the concepts for a wide range of operating conditions. This should aid in an evaluation of the relative merits of each concept to satisfy various mission requirements.

## 1.0 INTRODUCTION

The maximum allowable  $\text{CO}_2$  partial pressure for future manned space programs has been set at 3.0 mm Hg. This has required an evaluation of all  $\text{CO}_2$  management concepts capable of meeting the 3.0 mm Hg or less constraint. Ten concepts which have potential for meeting this requirement are listed below:

- o steam desorbed solid amines
- o vacuum desorbed solid amines
- o carbonation cell
- o hydrogen depolarized cell
- o solid electrolyte
- o liquid absorption
- o electrodialysis
- o molten carbonate
- o membrane diffusion
- o mechanical freezout

The above-mentioned concepts are in various stages of development. The steam desorbed reins concept has been tested in the 90-day manned simulator run. Extensive development work has been performed on the hydrogen depolarized cell concept for use in the Space Station Prototype (SSP) EC/LS being developed for NASA Manned Spacecraft Center (MSC). The molten carbonate concept is an example of a concept for which many design problems must be solved before a viable design is evolved.

In order to assist in the evaluation of the relative merits of each concept, computer subroutines have been developed for simulating the performance characteristics of the concepts.

The subroutines have been integrated into the G-189A Generalized Environmental Control computer program. A brief description of this computer program is contained in Appendix A of this report. Using the program, each concept can thus be evaluated for a wide variety of operational design conditions. The following conditions have been specified as design parameters:

o cabin total pressure	10 - 14.7 psia
o crew size	2 - 12
o dry bulb temperature	65 - 75°F
o wet bulb temperature	46 - 57°F
o $O_2$ partial pressure	3.1 to 3.5 psia
o cabin diluent gas	nitrogen
o gravity conditions	0 - 1.0 g
o $CO_2$ production rate	1.9 to 3.0 lb/man-day
o mission time	0.5 to 10 years

A generalized rather than specific approach has been used in preparing the simulation of the concepts. A typical concept was modeled by breaking up the subsystem into a series of functional components. These functional components might be an absorbing or desorbing bed, several heat exchangers or dehumidifiers, control valves, fans, etc. Existing G189A subroutines are available for simulating many of the functional components. New subroutines were prepared when required. For those components which have a common function in more than one concept, a single routine was prepared which could be used in simulating both concepts. For example, the same routine is used for simulating the absorption phase of operation for both the steam desorbed and vacuum desorbed resin concepts.

The subroutines used, order in which they are solved, sources of flow to a component are specified as input data to the G189A program. Any arbitrary arrangement can be simulated. The program has a considerable amount of flexibility for reflecting subsystem design or operating changes.

The simulation of a  $CO_2$  concentrator using the G189A may require incorporation of additional coding to simulate interfaces between components. This results from the cyclical operation of many of the concepts. Time sequencing valves may change the direction of flow from one component to another. For instance, when absorbing a bed received its flow (air) from one source, but while desorbing the same bed receives its flow (steam) from another source. Thus coding may be necessary to interpolate tables specifying the cyclical operation

of the bed, alter the order of component solution, and change the source of flow. This coding may be incorporated into G189A subroutine GPOLY or into a special purpose subroutine to simulate the interface function.

The body of this report contains descriptions of the concepts and the methods used in simulating each concept. Sample problems which illustrate the simulations are discussed in Volume II of this report. Descriptions of the new subroutines prepared and a listing of program data input requirements for the sample problems are contained in the appendices of Volume II.

The methods of simulation described and the new subroutines prepared will allow comparative evaluation of the performance of each concept. In particular the capacity of a particular design for maintaining a 3.0 mm Hg CO<sub>2</sub> partial pressure may be evaluated. Parametric runs for specified conditions of cabin pressure, crew size, or CO<sub>2</sub> production rate, cabin air dry and wet bulb temperatures, gravity, and mission duration may be made. The impact of interfaces with other subsystems such as oxygen regeneration or water recovery can be determined. This should aid in selection of the optimum subsystem and suitable alternatives for a particular space mission.

## 2.1 STEAM DESORBED RESINS

### 2.1.1 Process Description

In this  $\text{CO}_2$  concentration process, cabin air passes through a granular bed of solid amine particles such as amberlite IR-45 resin. Since amines are weak bases, carbon dioxide (an acid gas) undergoes a weak chemical reaction with the sorbent and is therefore removed from the cabin air.

As more and more carbon dioxide absorbs in the resin, a point will finally be reached when the  $\text{CO}_2$  in the gas stream comes to equilibrium with the  $\text{CO}_2$  absorbed in the resin. At this time, the resin will have picked up all the  $\text{CO}_2$  it is capable of holding and must then be regenerated.

In the steam desorb resin concept, regeneration is accomplished by passing superheated steam through the bed. Trapped air in the void space between particles is first pushed out. After elution of the air, carbon dioxide is the main effluent. When the  $\text{CO}_2$  is essentially depleted, steam-breakthrough occurs. Regeneration is then completed.

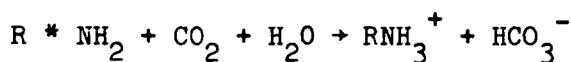
MSA Research Corporation, References 1 and 2, conducted fundamental studies on  $\text{CO}_2$  sorbents for NASA Langely Research Center. An ion-exchange resin, amberlite IR-45, manufactured by the Rohm and Haas Company proved to be durable and suitable for practical  $\text{CO}_2$  removal processes.

Hamilton Standard utilized surplus flight hardware from the MOL program to fabricate a solid-amine carbon dioxide concentrator. The performance of the unit was demonstrated in the 90-day manned test of MDAC, Reference 3.

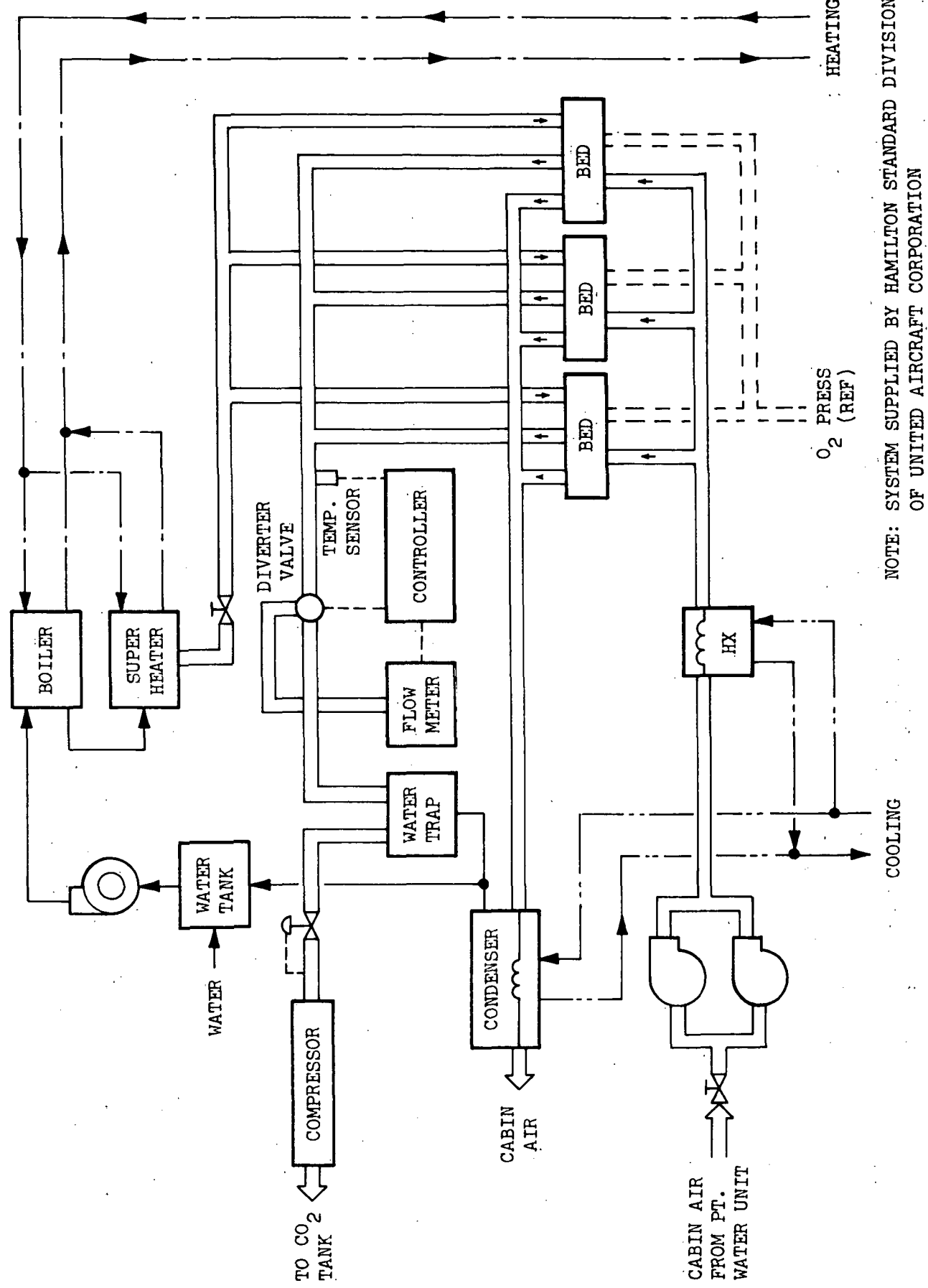
### 2.1.2 Process Operational Details

$\text{CO}_2$  is removed from cabin air by means of cyclic absorption/desorption in suitable granular amine resins. The chemical nature of the bonding between  $\text{CO}_2$  and these resins provides a  $\text{CO}_2$  removal method which is feasible for cabin

$P_{CO_2}$  levels of 3 mm Hg or less. Dynamic  $CO_2$  absorption and desorption processes, as well as equilibrium  $CO_2$  bed loading conditions, are extremely sensitive to the amount of water present. For example, for IR-45 resin, increases in bed water content up to as high as 40% weight result in corresponding increased absorption efficiencies (Reference 1). However, water vapor contents higher than 25% have been shown to cause excessive pressure drop and flooding. With the bed cooler than approximately 140°F the absorption process takes place according to the following relationship:



For steam desorbed resins, desorption is accomplished by flowing superheated steam into the bed in the axial direction. The steam condenses on the resin, heats the resin and displaces the  $CO_2$  and air. The process occurs in "chromatographic" fashion. That is, steam,  $CO_2$ , and air are found in individual zones which travel along the length of the bed. See Reference 1. The displaced  $CO_2$  is reabsorbed immediately ahead of the steam zone and the air is displaced ahead of the  $CO_2$ -rich zone. This chromatographic feature of the absorption process facilitates separation of  $CO_2$  from air and steam. Flows of the separate quantities of gas in each of the zones have associated physical properties which can be sensed and used in control schemes for diverting the  $CO_2$ -rich flow to the  $CO_2$  accumulator and also for diverting the air and steam flows back to the cabin via a condensing heat exchanger. Two of these properties which have been used in the steam desorbed resin  $CO_2$  concentrator for the LaRC/MDAC 90-day manned test are gas temperature and flow rate. See Figure 2.1-1.  $CO_2$  has a higher mass flow rate out of the bed than air does due in part to its higher molecular weight and, therefore, higher density. The increase in mass flow rate which occurs as the air zone is depleted and the  $CO_2$  zone elutes from the bed is sensed and a controller actuates a valve which diverts the  $CO_2$  to the  $CO_2$  accumulator. As the  $CO_2$  zone is depleted, an increase in gas temperature at the bed exit plane occurs as steam commences to leave the bed. This temperature is sensed and the control valve is actuated to divert the flow back to the cabin return line. The effluent steam is condensed in the



NOTE: SYSTEM SUPPLIED BY HAMILTON STANDARD DIVISION  
OF UNITED AIRCRAFT CORPORATION

FIGURE 2.1-1 NASA/MDAC 90-DAY MANNED TEST  
AMINE RESIN- $\text{CO}_2$  CONCENTRATOR SYSTEM

condensing heat exchanger in this line and the resulting condensate is returned to the water boiler. With steam desorbed resins the desorption phase of the process generally occurs at total gas pressures in the vicinity of cabin pressure. The pressure of the  $\text{CO}_2$ -rich gas leaving the bed is raised in a compressor to a pressure slightly in excess of  $\text{CO}_2$  accumulator pressure. Since accumulator pressures are often in the order of 50 psia or less, the required compressor pressure ratio and associated power are considerably less than they are for  $\text{CO}_2$  concentrator methods which utilize vacuum desorption.

Following desorption, the beds are hot and moist. Cabin atmosphere entering a bed during the absorption phase of the process is maintained at a suitable inlet temperature (65°F - 85°F) and the inlet humidity is maintained above a lower limit (~ 35% RH). Initially this entering air is heated by the hot moist bed. Heat is removed from the air in evaporating moisture from the bed. When desirable operating conditions are achieved, the amount of water condensed and partially absorbed in the bed during the desorption phase is exactly balanced by that evaporated during the absorption phase and the water content in the bed during absorption remains high enough to enhance  $\text{CO}_2$  absorption.

Figure 2.1-2 shows representative performance data for the steam desorbed resin  $\text{CO}_2$  concentrator used in the LaRC/MDAC 90-day manned test. These data were recorded during "two-bed operation". That is, two of the three available absorption beds are operating and the adsorption and desorption cycles were of equal duration. The lower curve shows the mixed  $\text{P}_{\text{CO}_2}$  downstream of the two absorption beds. As shown, the effluent  $\text{P}_{\text{CO}_2}$  drops rapidly at the start of the absorption phase, reaches a minimum value, and then rises with a plateau characteristic observed partway through the  $\text{P}_{\text{CO}_2}$  rise. This plateau characteristic was also reported in Reference 1. Again, in Figure 2.1-2 it is seen that most of the absorption occurs early in the absorption phase. The latter portion of the absorption phase was mainly used in drying the bed prior to the next desorption phase.

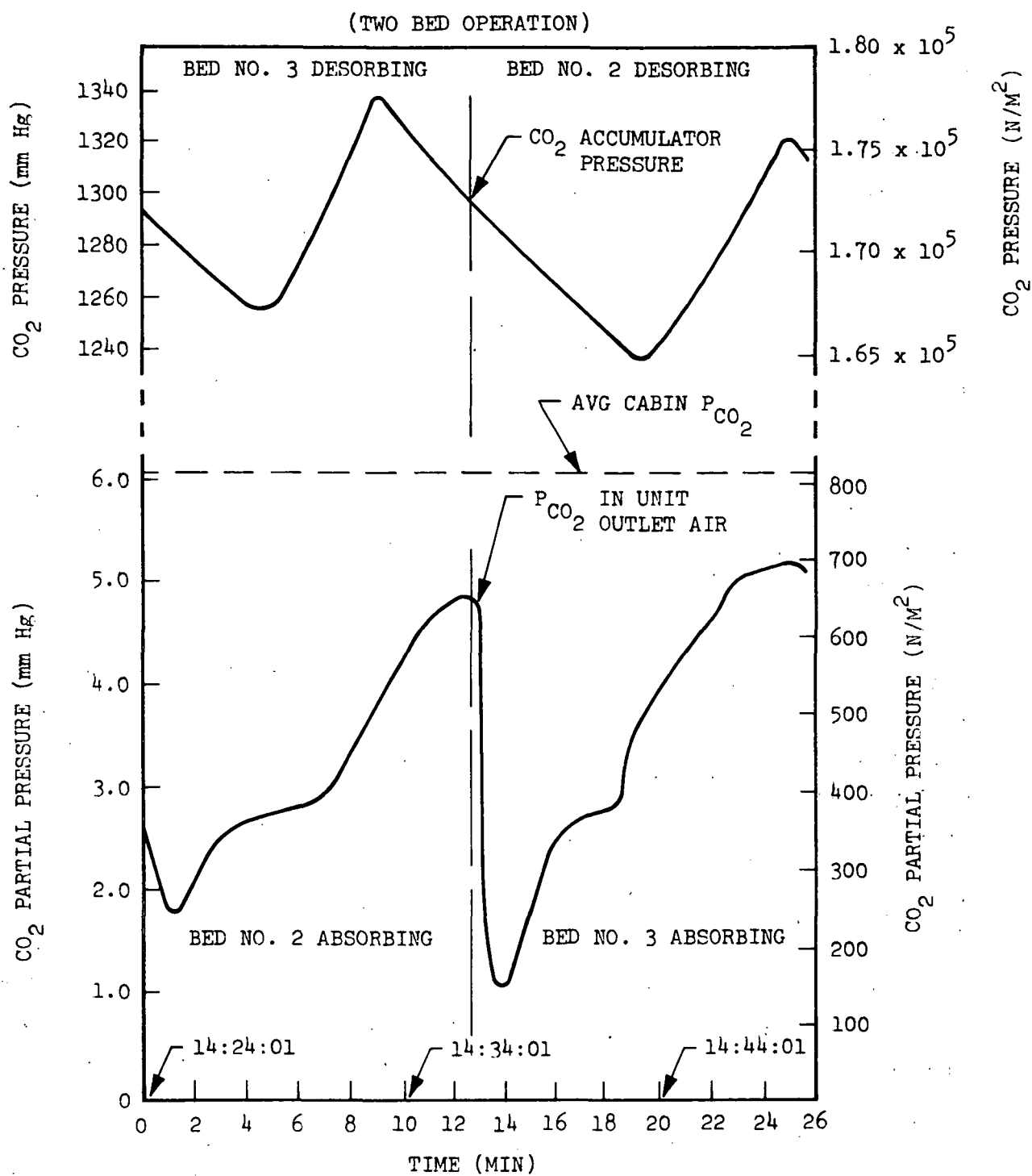


FIGURE 2.1-2 NASA/MDAC 90-DAY MANNED TEST  
AMINE RESIN CO<sub>2</sub> CONCENTRATOR PERFORMANCE

The upper curve on Figure 2.1-2 shows the  $P_{CO_2}$  in the accumulator. The negative slope portions of the curve are due to  $CO_2$  removal for supply to the Sabatier reactor. The positive slope portions are due to  $CO_2$  concentrator desorption. As shown in Figure 2.1-2 when Bed No. 2 is absorbing, Bed No. 3 is desorbing. From the earlier discussion concerning steam desorption, it is apparent that during the initial portion of the desorption phase air in the bed is eluted and flows back to the cabin. The  $CO_2$  zone is subsequently eluted and during this portion of the desorption phase flow is directed to the  $CO_2$  accumulator. This results in the positive slopes shown for accumulator pressure changes in Figure 2.1-2. Following elution of  $CO_2$ , steam flows out of the bed and the effluent is again diverted back to the cabin via the condensing heat exchanger. During this portion of the desorption phase, the  $P_{CO_2}$  in the accumulator again decreases due to the demand of the Sabatier reactor.

### 2.1.3 Simulation of Concept

The simulation of this concept is performed by dividing the subsystem into functional components, suitably connecting the components, and incorporating interface and control logic into GPØLY. Figure 2.1-3 is a schematic for the G-189A components required for simulation of a typical subsystem. The subroutines used are shown in parenthesis on the figure.

Gas from the cabin is supplied to the subsystem by component 14 (ALTCØM). This flow is circulated by FAN component 4 to bypass valve 5 (SPLIT). The flow not bypassing goes to absorbing bed component 6 (CØSØRP). This component simulates a solid amine's bed which removes  $CO_2$  from the cabin airstream. Since the bed is relatively wet with respect to the cabin air, moisture is picked up by the airstream. This moisture is removed by condensing heat exchanger component 7 (ANYHX). The coolant flow to this component is supplied by component 17 (ALTCØM). The dehumidified air then passes through a charcoal trap, component 8, which removes odors picked up in the amine's bed. The charcoal trap is simulated by subroutine ADSØRB.

While component 6 is removing  $\text{CO}_2$  from the cabin airstream, component 16 (CØSØRP) is being purged with superheated steam to drive off  $\text{CO}_2$  absorbed previously. Components 6 and 16 operate in a cyclic manner. While 6 is absorbing, 16 is desorbing. Steam to the bed is supplied by steam generator component 15. This component is simulated by a newly prepared subroutine SMGEN. Feed water to this component is pumped by metering pump 19 (PUMP) from water accumulator component 10 (TANKG). Condensate from heat exchanger components 7 and 12 is recirculated to this accumulator tank. Component 20 uses a new subroutine H2OSUM to sum up the flows from these two sources. Makeup water to the accumulator is supplied by feed water tank component 9 (TANKG).

The  $\text{CO}_2$ -steam mixture from the desorbing resin bed 16 is pumped by compressor 11 (FAN) through condensing heat exchanger component 12 (ANYHX). Coolant for this heat exchanger is supplied by component 18. De-humidified  $\text{CO}_2$  from the heat exchanger is pumped to accumulator component 13 (TANKG).

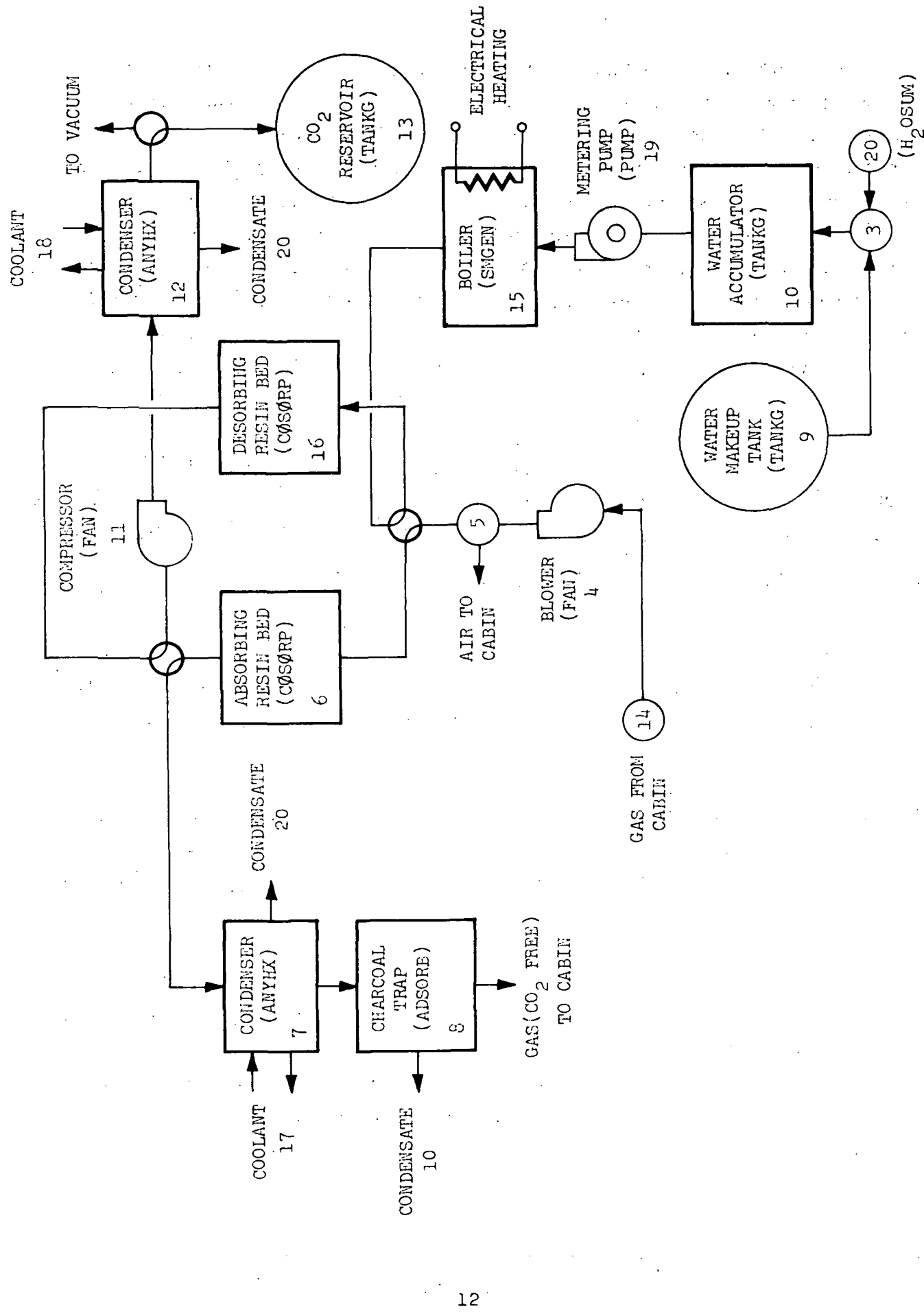


FIGURE 2.1-3 G189A SIMULATION OF A TYPICAL STREAM DESORBED SOLID AMINE  $\text{CO}_2$  CONCENTRATOR

## 2.2 VACUUM DESORBED SOLID AMINES

### 2.2.1 Process Description

This concept uses a solid amine resin bed to absorb  $\text{CO}_2$  from a spacecraft atmosphere. The bed is regenerated at suitable time intervals by the combined effects of heat and vacuum. The  $\text{CO}_2$  driven off in the bed is pumped to an accumulator for storage or usage by another subsystem. The accumulated gas may be dumped overboard or fed to an oxygen regeneration or propulsion system.

A prototype system using a proprietary resin designated as Gat-O-Sorb is described in Reference 4. The reported advantages of this system are that no predrying of the gas is necessary prior to carbon dioxide absorption and only moderate regenerative conditions ( $180^\circ\text{F}$  and 40 mm Hg) are necessary. One possible disadvantage of this system is that a considerable amount of water is also carried off by the vacuum pumping system during desorption cycle. Reference 4 reported a weight ratio of between 0.1 and 0.5 lb  $\text{H}_2\text{O}$ /lb  $\text{CO}_2$  collected during desorption. In reference 2 it was reported that for vacuum desorbed IR-45 solid amine resin, water is desorbed ahead of  $\text{CO}_2$ . Here a 20% bed water content was necessary to obtain a 2% value of  $\text{CO}_2$  bed loading. Thus, up to 10 lb  $\text{H}_2\text{O}$  may be desorbed/lb  $\text{CO}_2$ . This could pose a significant water removal problem.

Figure 2.2-1 shows a schematic of a prototype Gat-O-Sorb process. The unit was found to remove 0.41 lb  $\text{CO}_2$ /hr with a total resin weight of 30 lbs. The unit was tested through 91 different operating cycles without indication of absorbent deterioration.

The process shown in Figure 2.2-1 may be described as follows:  $\text{CO}_2$  is removed from the process gas in one bed while absorbed  $\text{CO}_2$  is being removed in the other bed. Two positions, four port valves are used to alternately reverse the bed functions. A centrifugal blower drives process gas through the absorbing bed, and a vacuum pump purges the desorbing bed. The beds are heated or cooled by tube-and-fin heat exchangers inside each canister and

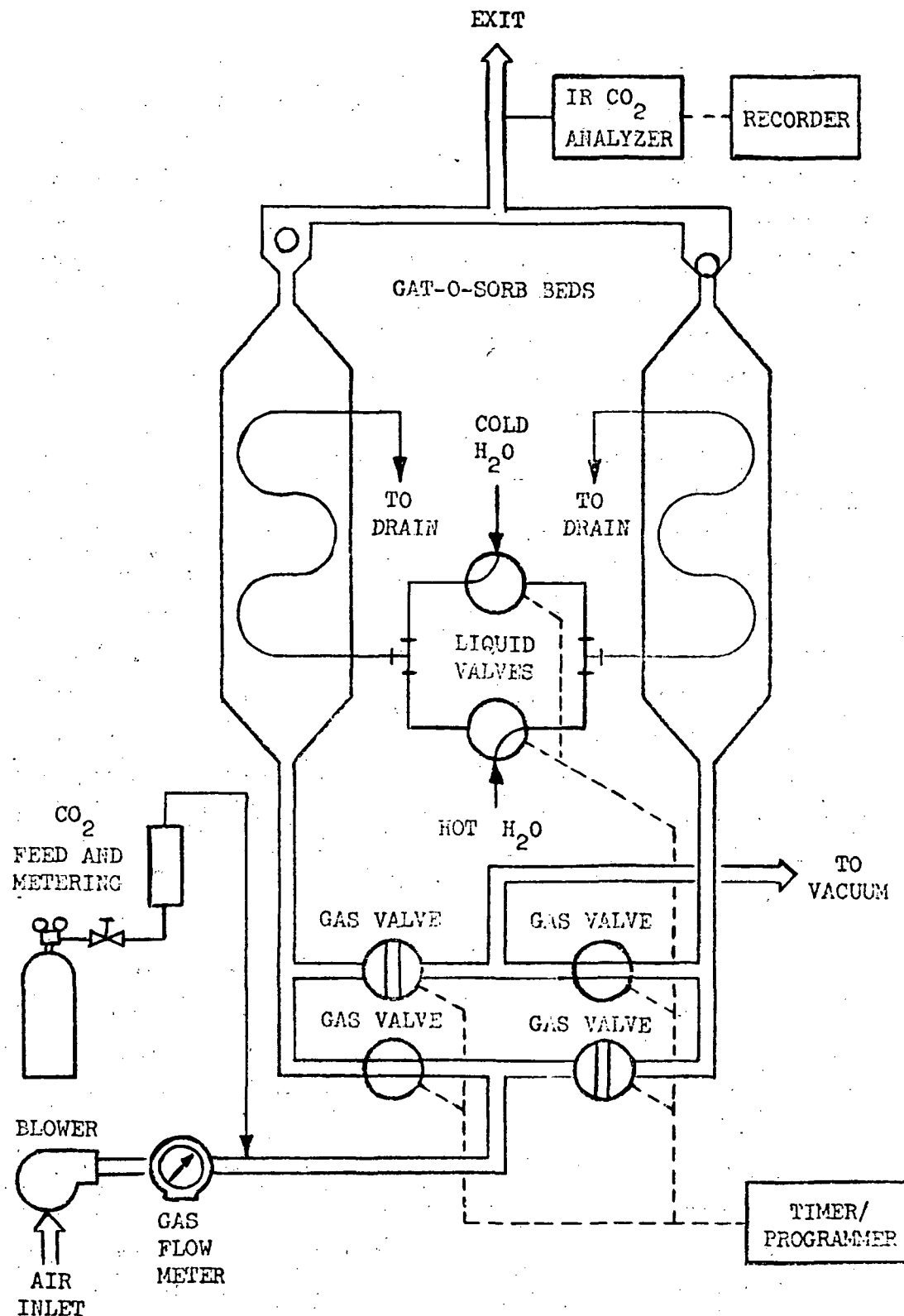


FIGURE 2.2-1 FLOW DIAGRAM OF BENCH SCALE  
GAT-O-SORB PROCESS

in direct contact with the adsorbent particles. When absorbing, cool water is circulated through a bed. When desorbing, hot fluid is used.

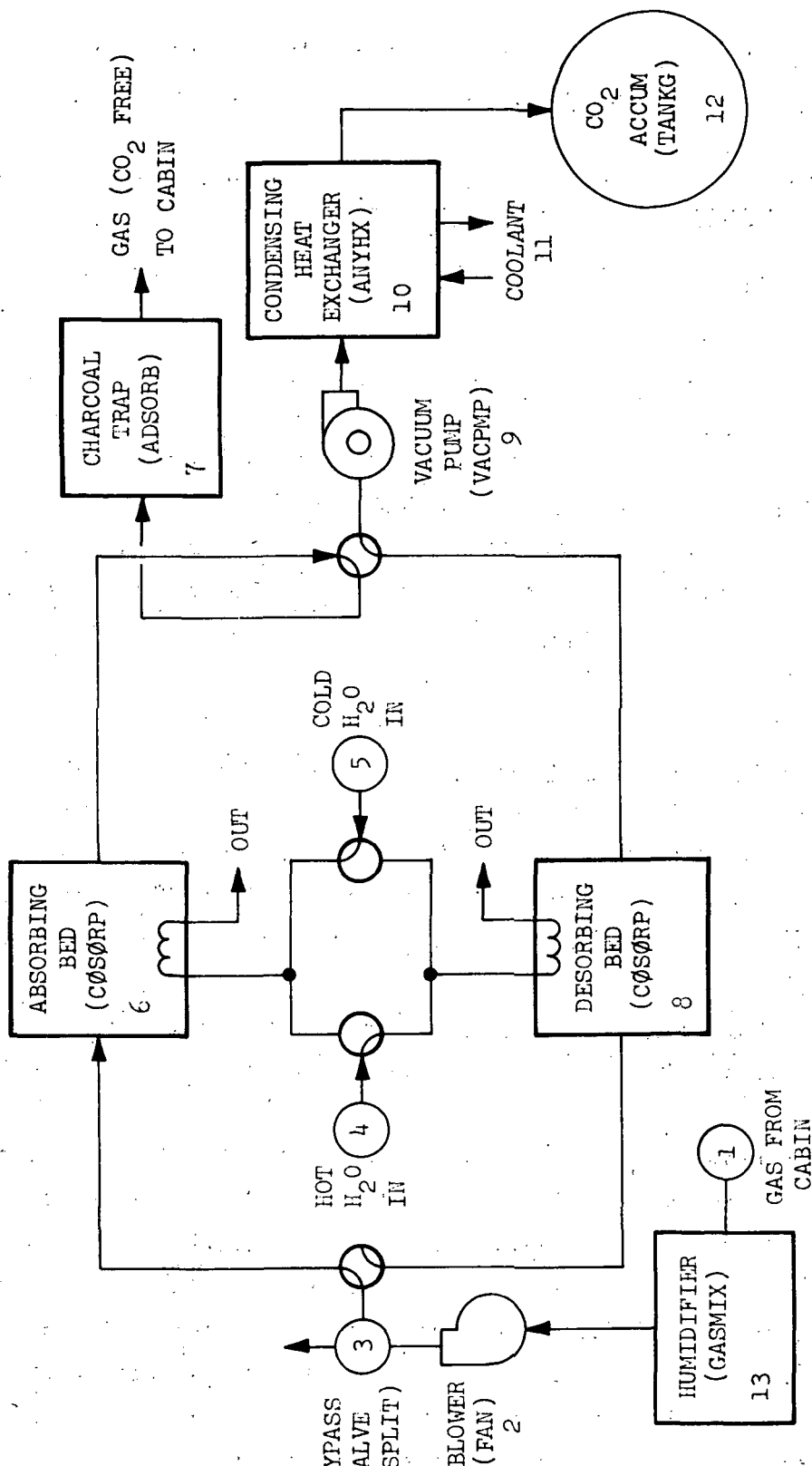
Below inlet relative humidities of 50%, the adsorbent was found to gradually dehydrate and lose its capacity for  $\text{CO}_2$  absorption. RH above 50% was found not be harmful to the process. RH below 50% could be tolerated for exposure times of several hours.

### 2.2.2 Simulation of Concept

The thermal/vacuum desorbed amines concept for  $\text{CO}_2$  removal will be simulated by suitably connecting G-189A components which simulate individual components or functions of the concentrator. Figure 2.2-2 illustrates the G-189A components required for a typical subsystem. The subroutines used for each component are given in parenthesis.

Gas from the cabin is supplied by component 1 (ALTCØM). The gas is circulated to the subsystem by blower component 2 (FAN). The gas flows to component 3 (SPLIT) which controls the amount of gas bypassing the subsystem. Flow then passes through a solid amines resin bed component 6 (CØSØRP) where  $\text{CO}_2$  is removed by absorption. Cooling fluid (water) flows from component 5 (ALTCØM) through the bed's integral heat exchanger. The coolant is required for removing the heat of absorption and the thermal energy stored in the bed during the thermal/vacuum desorption cycle.  $\text{CO}_2$  free gas flows from the bed to charcoal trap component 7 (ADSORB) and back into the cabin.

While component 6 is absorbing  $\text{CO}_2$ , component 8 (COSORP) is being desorbed of  $\text{CO}_2$  collected previously. Desorption is affected by the combined effects of heat and vacuum. The heat is supplied by hot water from component 4. Desorbed  $\text{CO}_2$  plus water vapor is transferred by vacuum pump component 9 (VACPMP) through condensing heat exchanger component 10 (ANYHX). Water vapor picked up during desorption is removed in this component. The dehumidified gas then flows to accumulator tank component 12 (TANKG) for storage or use by an oxygen regeneration subsystem.



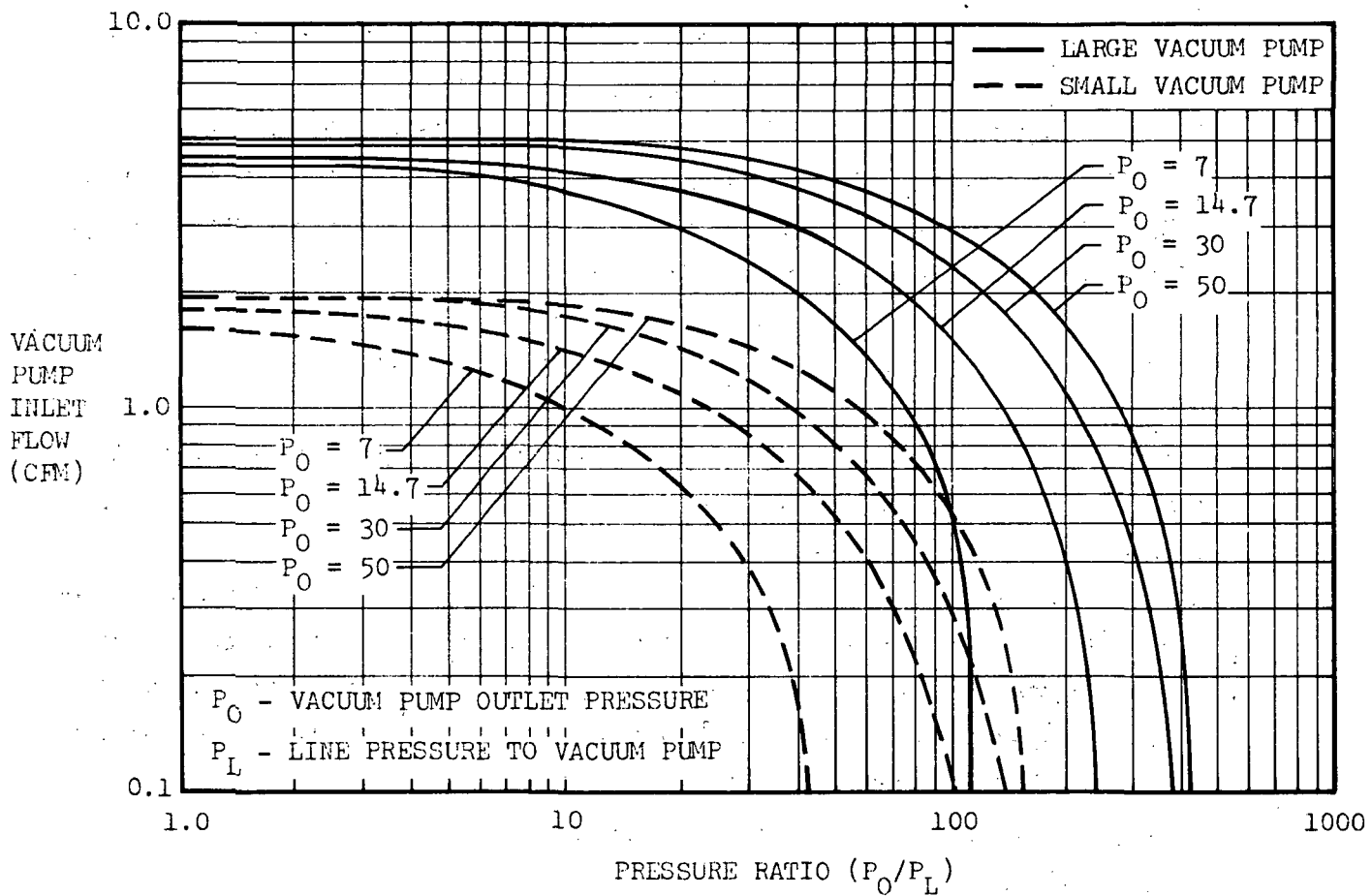


FIGURE 2.2-3 VACUUM PUMP CHARACTERISTICS

## 2.3 CARBONATION CELL

### 2.3.1 Process Description

The carbonation cell concentrator is an electrochemical device for collecting  $\text{CO}_2$  from a cabin atmosphere. The process operates in a continuous rather than cyclic manner. The  $\text{CO}_2$  collected is free of diluent gas contamination. Figure 2.3-1 illustrates the major components of a typical carbonation cell collector. Moist air is circulated into the cathode compartment of Stage I. An impressed voltage creates electrolytic reactions at the cell's two electrodes which are separated by an aqueous carbonate electrolyte held within an asbestos matrix. The net effect of the reactions is to liberate  $\text{O}_2$  and  $\text{CO}_2$  at the cell's anode compartment. Purity ranges between 50 and 70 mole percent. Air depleted in oxygen and with negligible amounts of  $\text{CO}_2$  flows from the outlet of the cathode back to the cabin.

The gas freed at the anode is then transferred to Stage II which employs an aqueous acid electrolyte. An impressed voltage and accompanying electrolytic reactions create a liberation of only  $\text{O}_2$  at the anode of this stage.  $\text{CO}_2$  is concentrated at the cathode of this cell.

The concentrated  $\text{CO}_2$  stream from the Stage II cathode passes through a condenser/separator to remove water vapor gained through evaporation in the cells. A compressor is used to force the  $\text{CO}_2$  into a storage tank. Details on the operation of the I and II stages of the concentrator, which were abstracted from Reference 6 are given below:

#### First Stage (Carbonation Cell) Operation -

Process air flows into the cell cathode compartment where  $\text{O}_2$  and  $\text{CO}_2$  are absorbed by the cell electrolyte. Oxygen combines with water to form hydroxyl ions while  $\text{CO}_2$  reacts with hydroxyl ions to form carbonate ( $\text{CO}_3^{=}$ ) or bicarbonate ( $\text{HCO}_3^-$ ) ions. The  $\text{OH}^-$ ,  $\text{CO}_3^{=}$ , and  $\text{HCO}_3^-$  ions diffuse through the electrolyte to the anode compartment. These ions react at the anode to liberate  $\text{CO}_2$  and  $\text{H}_2\text{O}$ . Figure 2.3-2 illustrates the electrochemical reactions at the anode and cathodes.

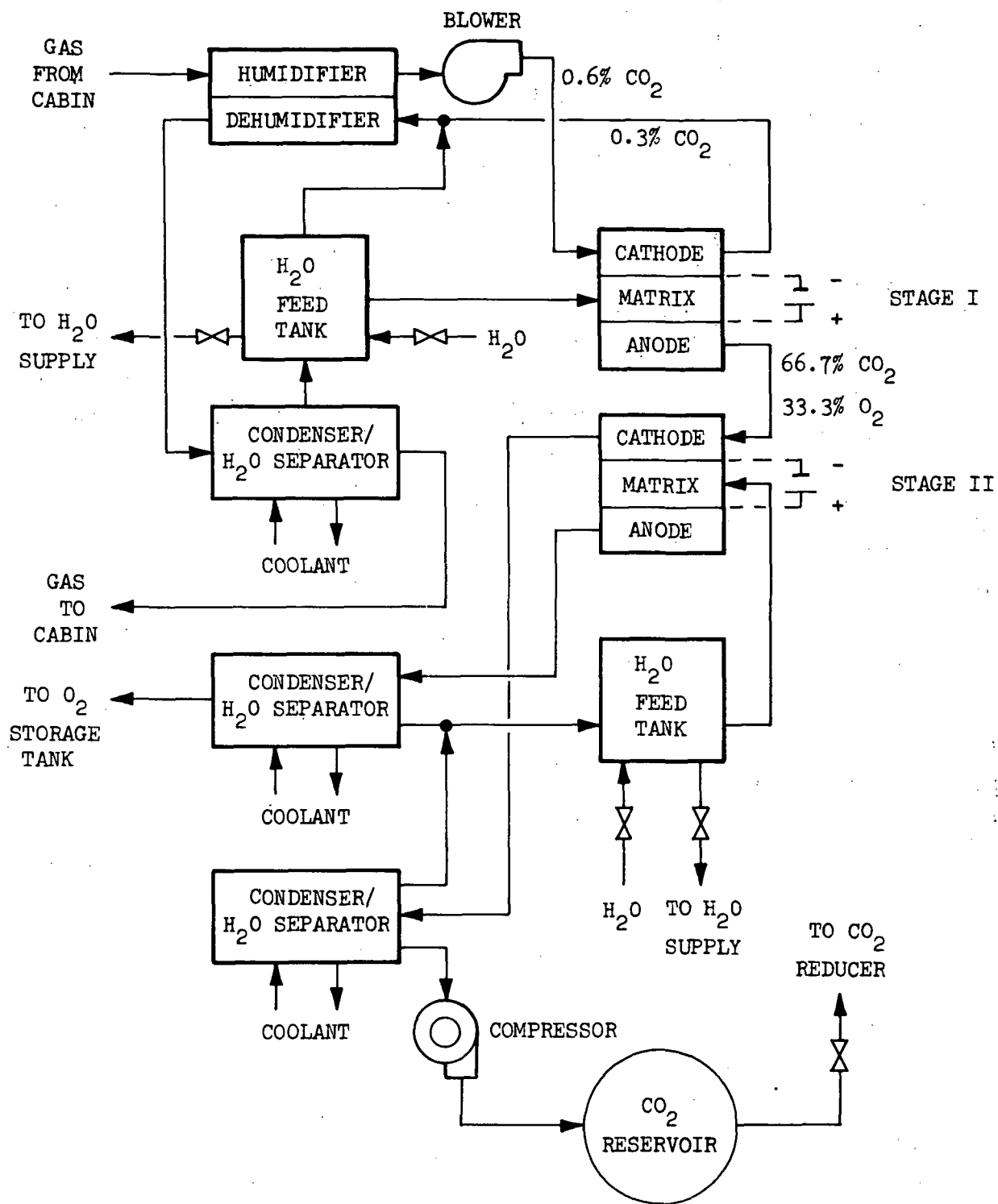


FIGURE 2.3-1 CARBONATION CELL CO<sub>2</sub> COLLECTOR

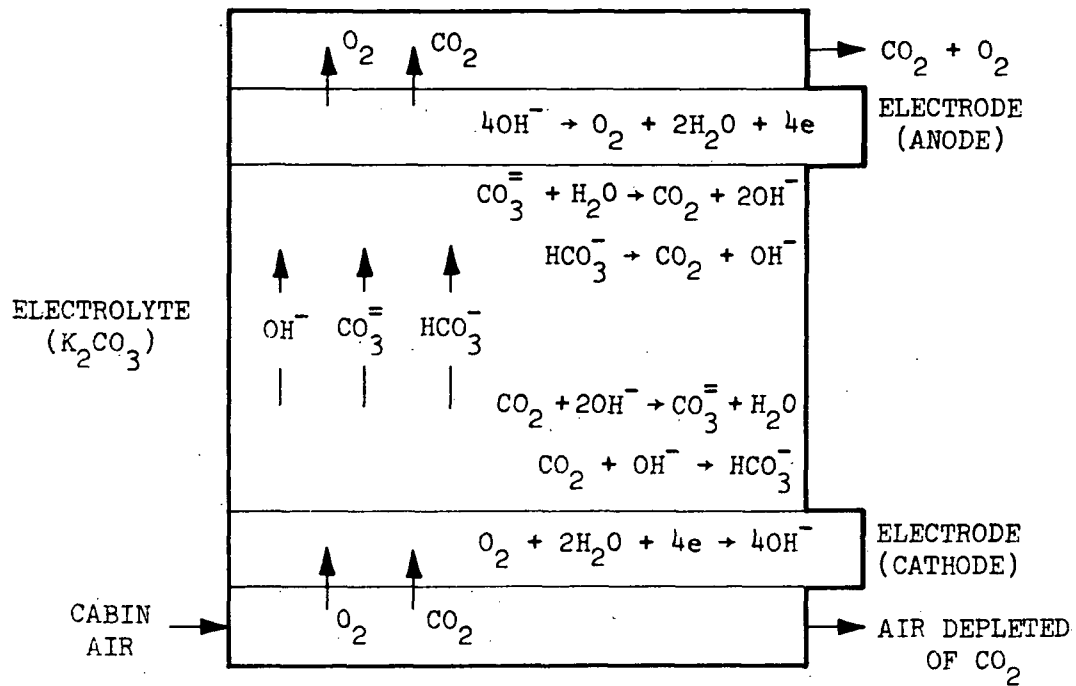


FIGURE 2.3-2 CARBONATION CELL STAGE 1 -  
SCHEMATIC REPRESENTATION

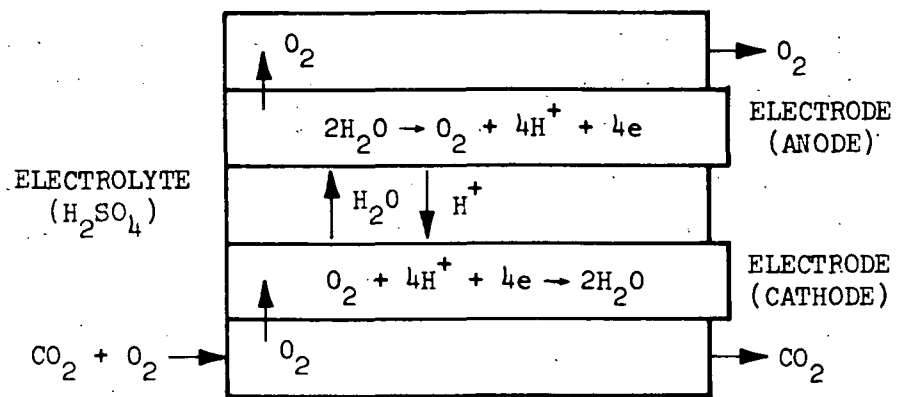


FIGURE 2.3-3 CARBONATION CELL STAGE II -  
SCHEMATIC REPRESENTATION

The electrochemical reactions vary significantly with carbon dioxide partial pressure in the cathode gas. For very low  $\text{CO}_2$  concentrations, only  $\text{OH}^-$  ions are formed and thus only  $\text{O}_2$  is liberated at the anode. At very high  $\text{CO}_2$  partial pressures, a large number of bicarbonate ions are formed to favor a high  $\text{CO}_2$  to oxygen ratio at the anode. At normal operating levels of 0.03 to 1.0%  $\text{CO}_2$ , most of the carbon dioxide is liberated through transference by the carbonate ions. At a current density of 40 amps/ $\text{ft}^2$  and a cell temperature of  $140^\circ$ , the  $\text{CO}_2$  transfer rate is approximately 5cc per amp-min. The anode gas concentration is over 55%  $\text{CO}_2$ .

#### Second Stage Operation -

$\text{CO}_2$  level could be boosted to a maximum amount of 80% through use of a second carbonate stage. However, a second stage employing an acid electrolyte was found effective in achieving a  $\text{CO}_2$  concentration of almost 100%. Here the active species is the hydrogen ion. Oxygen reacts with this ion at the cell cathode to form water which migrates to the anode. Here the water is decomposed to oxygen and hydrogen ions. Thus no  $\text{CO}_2$  is transferred in this stage and a high separation efficiency is achieved. Details on the cell reactions are shown in Figure 2.3-3. Using a design value of 50 amps/ $\text{ft}^2$  oxygen was found to be transferred at a rate close to the theoretical value of 3.5 cc (STP) per amp-min.

#### 2.3.2 Simulation of Concept

The simulation of the carbonation cell  $\text{CO}_2$  concentration subsystem is performed by dividing the subsystem into major functional components which are modeled by G-189A component subroutines. Figure 2.3-4 represents a typical subsystem. Process gas flow from the cabin is supplied by component 1 (ALTCOM).

A blower (FAN), component 2, forces process gas through the subsystem. Prior to entering the concentrator, the process gas flows through a humidifier (HUMID), component 3, where water vapor exchange takes place with the process gas leaving the first stage of the concentrator. The humidified process gas

then flows to the cathode compartment of the first stage, component 4 (CARCL1), of the subsystem. Process gas leaves the cathode compartment essentially free of  $\text{CO}_2$ . An  $\text{O}_2/\text{CO}_2$  mixture leaves the anode compartment. The purified process gas leaving the first stage flows back through compartment 3 (HUMIDT) to condenser/separator component 6 (ANYHX) prior to returning to the cabin.

The  $\text{CO}_2/\text{O}_2$  mixture from the anode compartment of the first stage flows to the cathode side of component 8 (CARCL2) which is the second stage of the concentrator.  $\text{CO}_2$  is obtained from the cathode side of this stage while  $\text{O}_2$  is obtained at the anode side.  $\text{CO}_2$  from the cathode side flows to condenser/water separator component 9 (ANYHX). The dehumidified  $\text{CO}_2$  is pumped by component 20 (FAN) to a  $\text{CO}_2$  reservoir component 21 (TANKG).  $\text{O}_2$  collected at the anode side of the second stage flows to condenser/water separator component 10 (ANYHX). The dehumidified  $\text{O}_2$  is pumped by component 22 (FAN) to accumulator component 23 (TANKG).

The condensate flows from condenser/water separator components 6, 9, and 10 are summed up by component 16 (H20SUM). The total condensate flow is pumped by component 17 (PUMP) to water storage tank component 18 (TANKG). This tank provides makeup feed for the two carbonation cell stages, components 4 and 8. The amount of makeup water required is calculated by GPOLY logic. This water is added to the subsystem at component 5 (GASMIX).

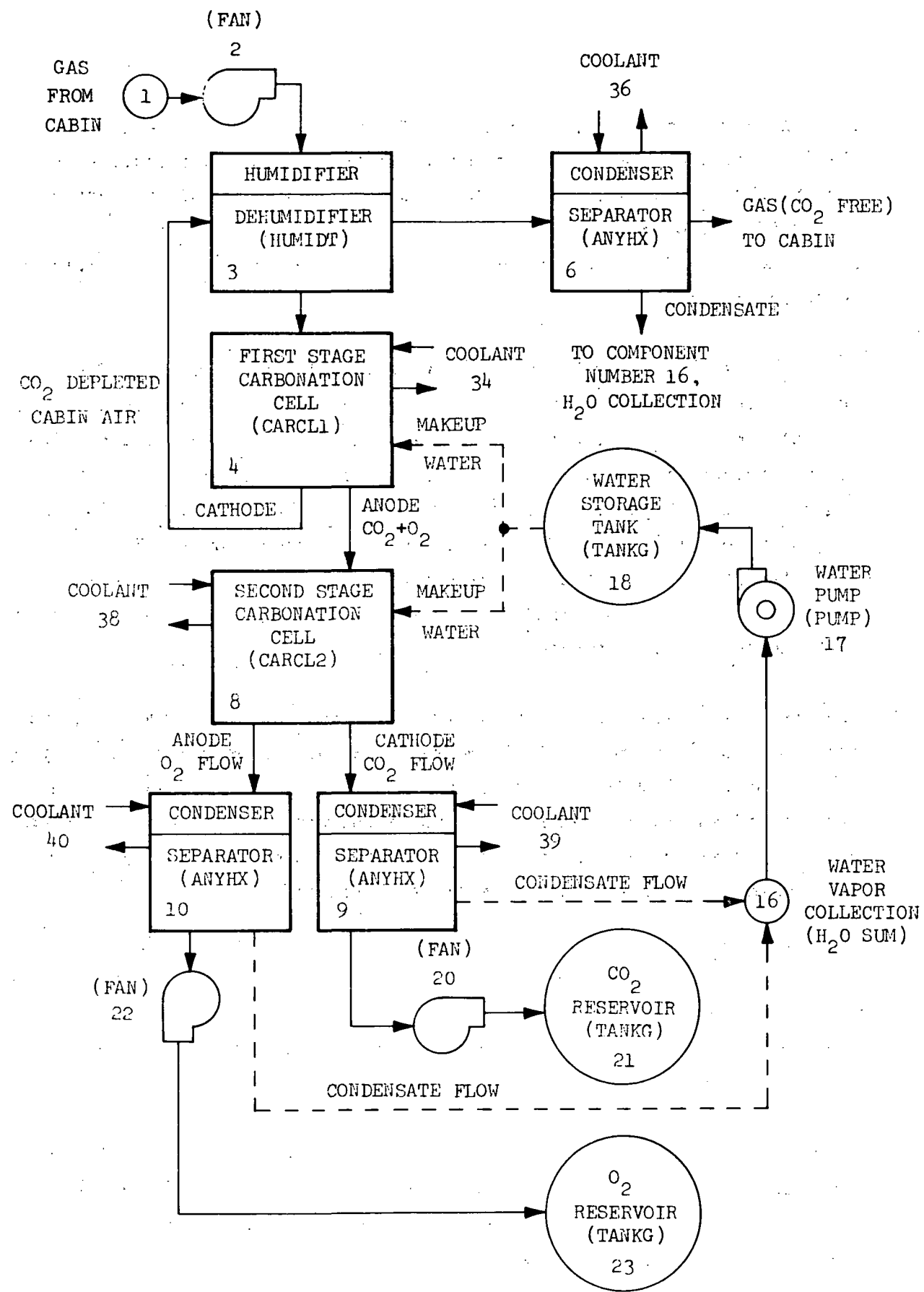


FIGURE 2.3-4 G189A CARBONATION CELL COMPONENT CONNECTION AND DEFINITION

## 2.4 HYDROGEN DEPOLARIZED CELL

### 2.4.1 Concept Description

The hydrogen depolarized cell is an electrolytic process for  $\text{CO}_2$  concentration. The concept evolved from the carbonation cell concept. The process differs in that only one stage is required, and that hydrogen is introduced at the anode of the cell. The hydrogen serves to depolarize the cell to shift the chemical equilibrium in the direction of  $\text{CO}_2$  formation. The cell acts similar to a fuel cell since hydrogen and oxygen are consumed and electricity is generated. The electricity generated provides the energy required to create the electrolytic reactions which cause the separation of  $\text{CO}_2$  from  $\text{O}_2$ . A considerable amount of design effort and development testing have been conducted for the concept over the past seven years (1965-1972).

The process has a considerable amount of flexibility in the range of  $\text{CO}_2$  partial pressures over which it can operate. The removal rate can be modulated if desired. The unit operates continuously requiring no regeneration. In addition the unit is reported to have a low equivalent weight compared to the other concepts for  $\text{CO}_2$  removal (Reference 7).

Figure 2.4-1 illustrates the reactions occurring in the cell.  $\text{Cs}_2\text{CO}_3$  electrolyte is used rather than the  $\text{K}_2\text{CO}_3$  used in the carbonation cell. Moist cabin air is fed to the cathode where oxygen reacts to form  $\text{OH}^-$  ion. These ions react with  $\text{CO}_2$  to form carbonate ions. The air leaving the cathode compartment thus is depleted in both  $\text{O}_2$  and  $\text{CO}_2$ . The  $\text{CO}_3^{=}$  ions migrate in the electrolyte to the anode where they react with water to generate  $\text{CO}_2$ . Hydrogen introduced at the anode reacts with  $\text{OH}^-$  ions to shift the anode reactions in the direction favoring formation of  $\text{CO}_2$ .

The  $\text{CO}_2$  liberated at the anode is free of  $\text{O}_2$  but mixed with  $\text{H}_2$ . The cell can operate effectively with percentages of  $\text{H}_2$  varying from 20 to 90%. This mixture can be controlled to achieve the mix ratio desired for feed to a Sabatier  $\text{CO}_2$  reduction process.

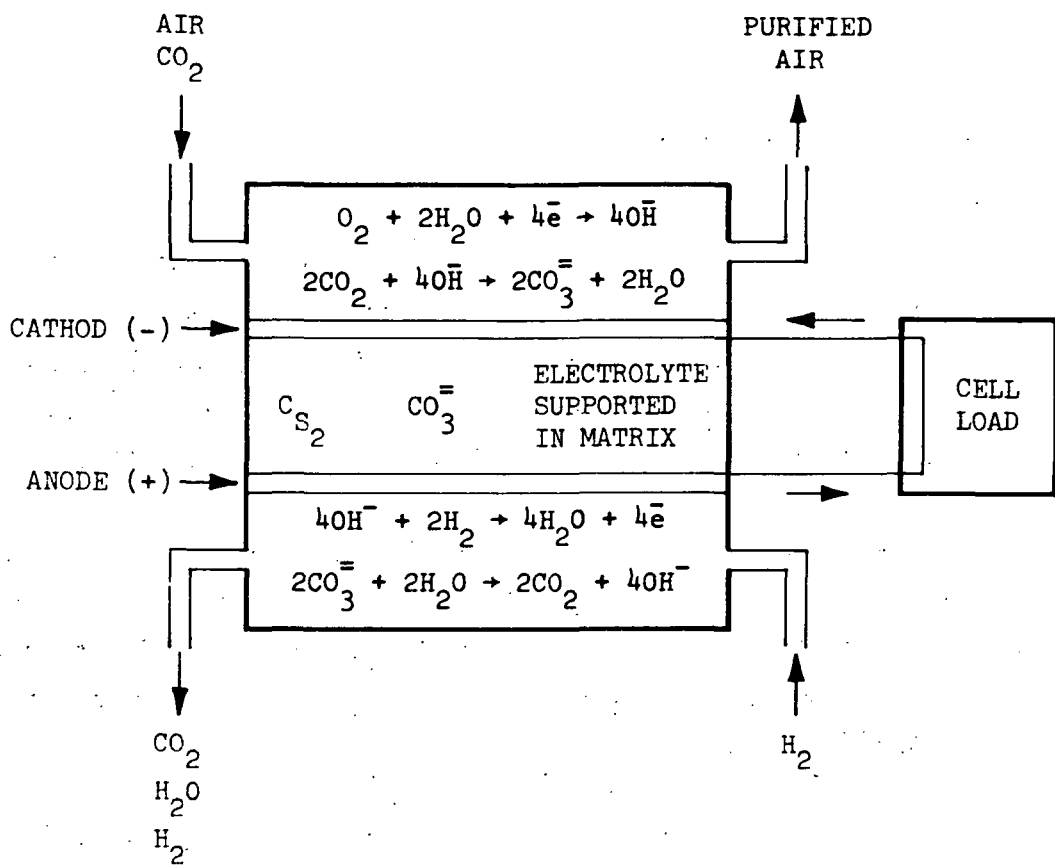


FIGURE 2.4-1 HYDROGEN DEPOLARIZED CELL

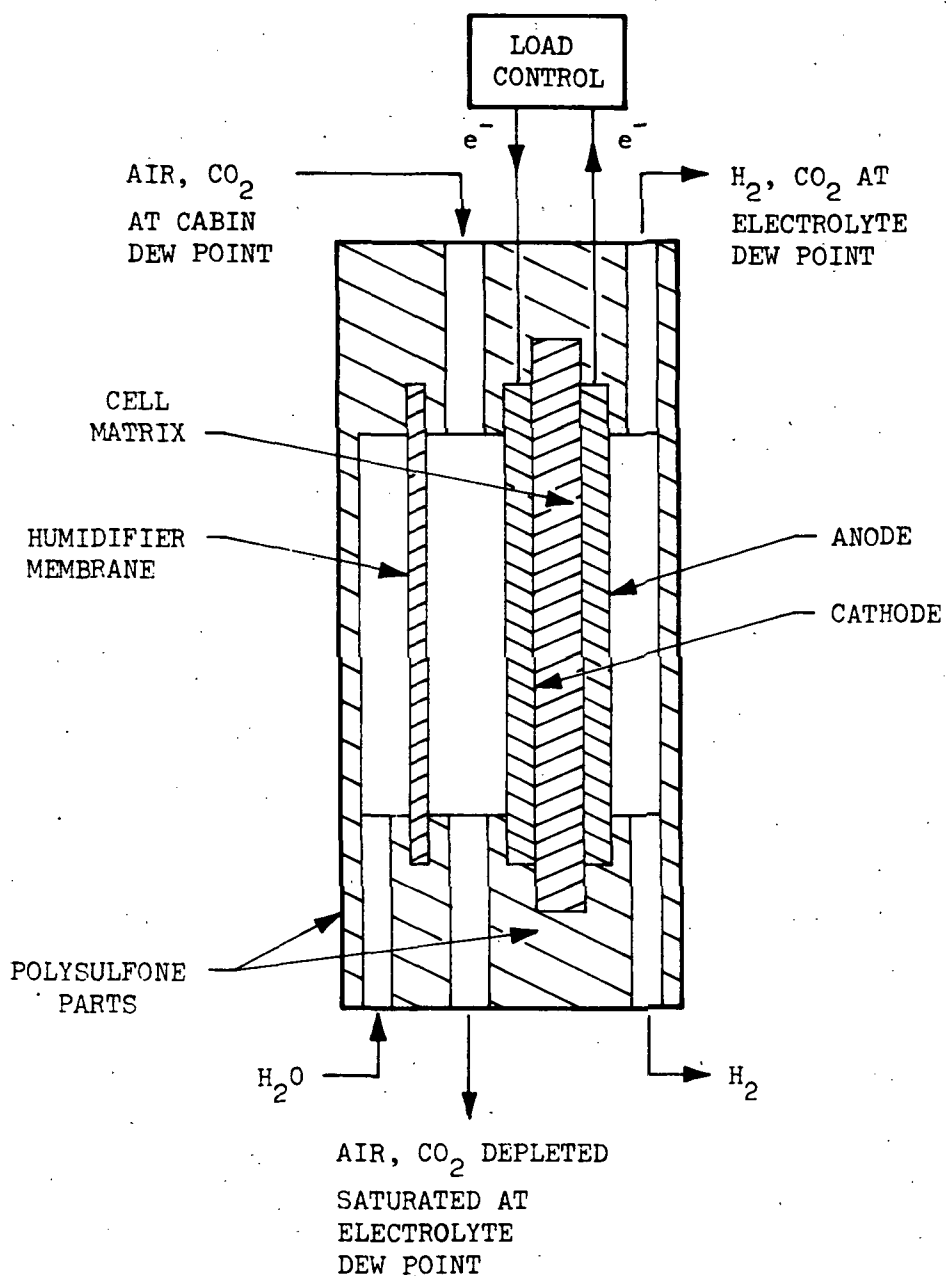


FIGURE 2.4-2 HDC SCHEMATIC

The concept incorporates an integral dehumidifier/humidifier to prevent dry out of the cells. Figure 2.4-2 shows a cross section of a typical cell. Further details on the operation of the cell are given in reference 7. Other information is provided in references 8, 9, and 10. A detailed analytical model for the cell reactions is described in reference 11.

Thermal control of the cell temperature is accomplished through evaporation of water into the product streams.

#### 2.4.2 Simulation of Concept

Figure 2.4.3 illustrates the functional components required for simulating the SSP Concentrator (Reference 12). The functions of each component are described as follows:

Air from the cabin is drawn through a dehumidifier component 2 (ANYHX). The dehumidifier is necessary to control air relative humidity within specified bounds. This control is necessary to prevent flooding or drying out of the cell electrolyte. The air then is drawn by blower component 3 (FAN) into the cathode compartment of hydrogen depolarized cell component 5 (H2DPØL). Here the  $\text{CO}_2$  is scrubbed out by electrochemical reactions. The purified gas leaves the cell, flows through filter component 7 (ADSORB) which removes trace contaminants and returns to the cabin.

Hydrogen flow to the anode compartment is supplied by storage tank component 8 (TANKG). The hydrogen passes through filter component 9 (ADSORB) prior to entering the cell. In the anode compartment, hydrogen reacts with  $\text{OH}^-$  to generate water. The water reacts with  $\text{CO}_3^{=}$  ions to regenerate  $\text{CO}_2$ .  $\text{CO}_2$  and unreacted  $\text{H}_2$  flow out of this compartment into storage tank component 10 (TANKG). This tank serves as a source of flow to a Sabatier reactor oxygen regeneration subsystem.

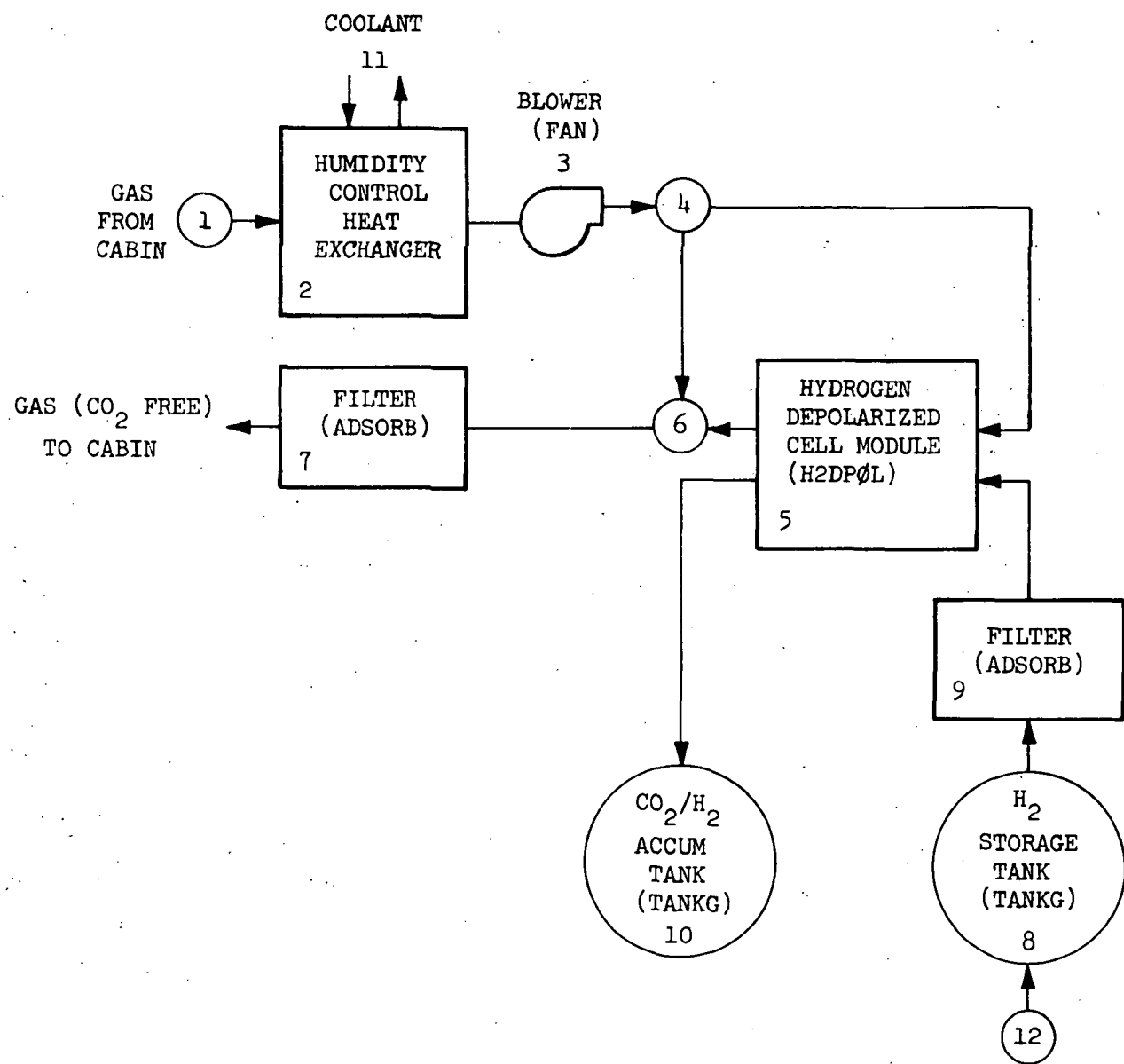


FIGURE 2.4-3 G-189A SIMULATION HYDROGEN DEPOLARIZED CELL CONCENTRATOR

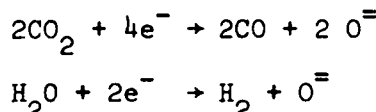
## 2.5 SOLID ELECTROLYTE

### 2.5.1 Process Description

Although the solid electrolyte process is conventionally categorized as a  $\text{CO}_2$  reduction scheme, and therefore not in the same functional category as the previous  $\text{CO}_2$  management concepts, it has some unique features that warrant discussion.

The solid electrolyte process (see References 13 and 14) in conjunction with a CO disproportionation reactor results in the reduction of  $\text{CO}_2$  to carbon and oxygen. A small amount of water vapor in the  $\text{CO}_2$  feed, which enhances the main reaction, is simultaneously electrolyzed to hydrogen and oxygen. Reference 15 points out that close coupling of this system with a carbon dioxide concentrator which generates humidified carbon dioxide continuously would have operational advantages. All of the previous writeups on the various  $\text{CO}_2$  management concepts implicitly assumed that "dry"  $\text{CO}_2$  was the desired product, mainly because the Sabatier or Bosch reactions were envisioned as the next step. The reason for discussing the solid electrolyte process, therefore, is to emphasize that humidified  $\text{CO}_2$  might be the desired product from a  $\text{CO}_2$  concentrator in some trade-off studies.

The system is composed of cells consisting of a solid electrolyte mixture of 91.25 mole percent zirconia ( $\text{ZrO}_2$ ) and 8.75 mole percent yttria ( $\text{Y}_2\text{O}_3$ ). This solid electrolyte is situated between two platinum electrodes to which the electrolyzing potential is applied. The basic electrochemical separation process which occurs is illustrated in Figure 2.5-1. For a gas stream including carbon dioxide and water vapor the following reactions occur at the anode:



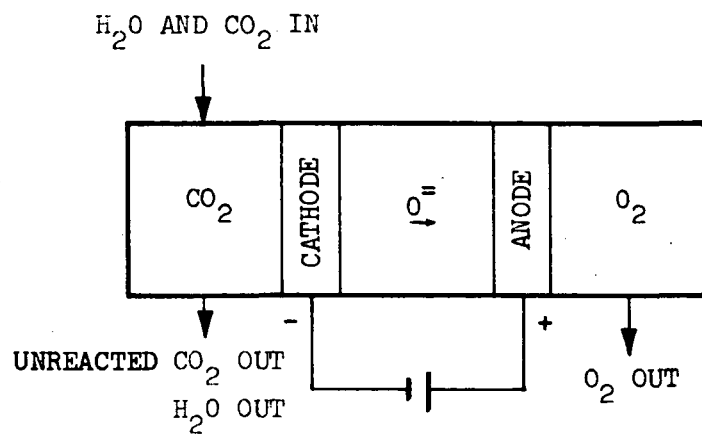


FIGURE 2.5-1 SOLID ELECTROLYTE CELL REACTIONS

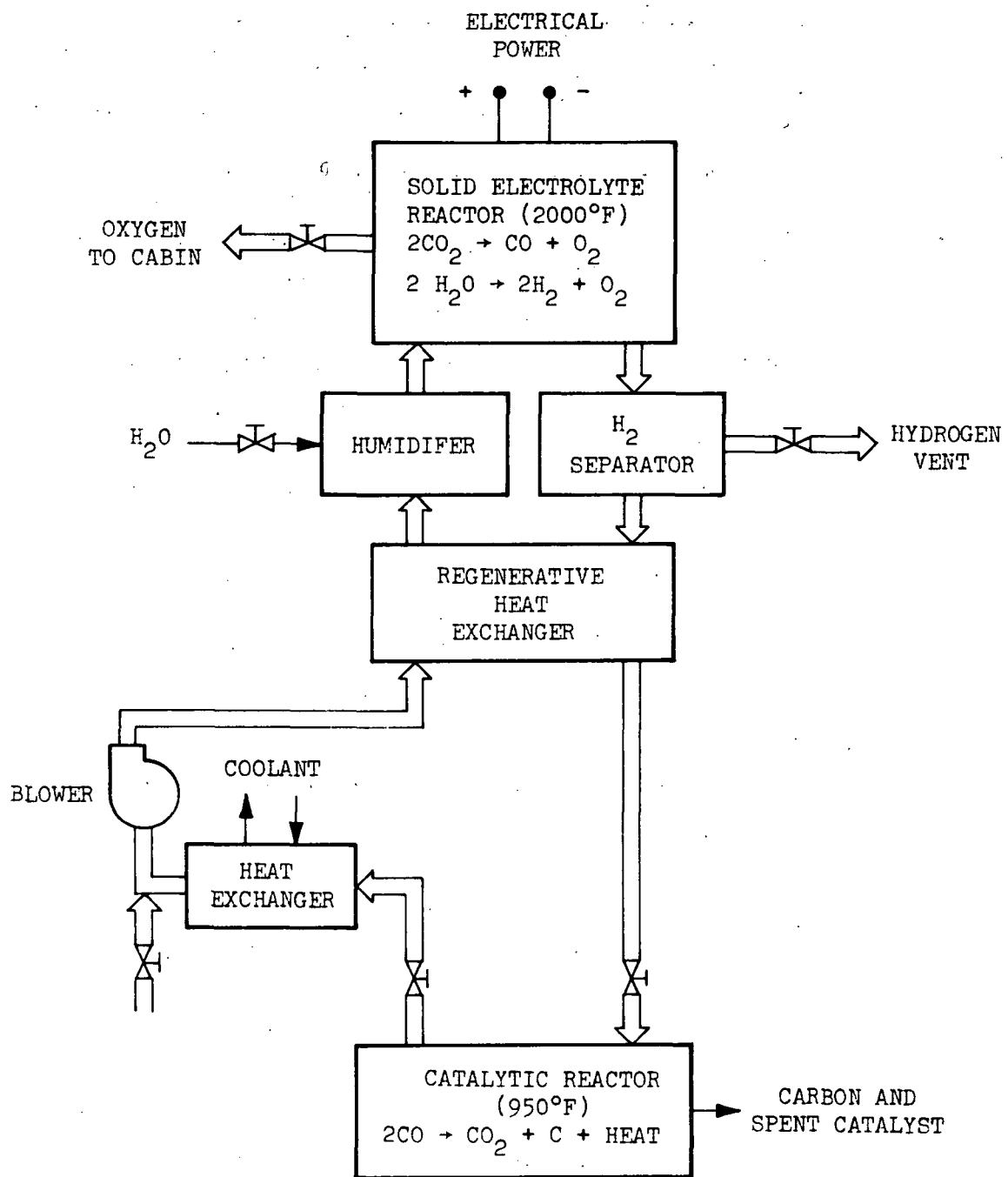


FIGURE 2.5-2 SOLID ELECTROLYTE SCHEMATIC

At a temperature of 525-700°C (1000-1300°F), the  $O^=$  ions will be transported across the oxide film by the influence of the potential gradient. The reactions are enhanced by the presence of  $H_2O$  in the gas stream. The oxygen ion then migrates under the influence of a potential field through vacancies in the crystal lattice of the solid electrolyte material to the anode, where the oxygen ion is converted to an oxygen atom. The solid electrolyte is essentially impermeable to non-ionic species (in particular it is impermeable to  $CO$ ) so that pure  $O_2$  is formed at the anode and may be sent to the cabin with no further processing other than cooling. The power consumption in the cell is split between energy required to decompose the  $CO_2$  and the resistance heating of the solid electrolyte material. As the predicted cell efficiency is thought to be good and the operating temperature high, this unit must be well insulated to prevent heat leakage which would decrease unit performance. An auxiliary heater in the cell tube is designed to bring the tube to operating temperature.

The free energy change involved in the decomposition of  $CO_2$  to carbon monoxide and to oxygen is 123 kcal/gram-mole of oxygen. This corresponds to a theoretical power requirement for a cell of 68.8 watts/kg of  $CO_2$  per day.

The mixture of  $CO$  and  $CO_2$  from the cell cathode is passed through a catalytic reactor which converts  $CO$  to  $CO_2$  (returned to the electrolytic cell) and to solid carbon. The free energy change in this reaction is 29 kcal/gram-mole of carbon. This corresponds to a heat dissipation requirement of 45 watts/kg of  $CO_2$  per day.

A flow diagram of a solid electrolyte system is given in Figure 2.5-2 which shows that after leaving the electrolyte cell, a separator is used to remove hydrogen from the gas stream. Also, a regenerative heat exchanger is used to cool the gas products to approximately 950°F, which is the operating temperature of the catalytic reactor. In the catalytic reactor, the carbon monoxide is dissociated to form carbon and carbon dioxide over a nickel or stainless steel catalyst. When the resultant carbon has built up to a high

level, a pressure switch will sense the increasing differential pressure and signal for a change of catalyst bed. The catalytic reaction is exothermic and no heating of this unit is necessary once the system has reached operating temperature. A heat exchanger is used to remove the excess heat of reaction from the gas stream. A blower draws the recycle and process gases through the regenerative heat exchanger and humidifier before returning them to the electrolytic reactor.

#### 2.5.2 Simulation of Concept

Two distinct cell designs have been fabricated and successfully tested. The first as reported in Reference 16 uses solid electrolyte discs between which the electrical potential is applied. The second which is reported in Reference 17 and 18 uses solid electrolyte tubes. Here the potential is applied at electrodes located on the inside and outside surfaces of the tubes. The second cell design differs from the first in that it incorporates a semipermeable palladium membrane for separating hydrogen from the exit products.

Relatively low concentrations of hydrogen in the inlet to the reactor have been found to increase the rate of carbon formation. Higher concentrations will shift the chemical equilibrium away from carbon formation. The semi-permeable membrane provides a means for regulating the concentration of hydrogen and thus carbon formation.

Figure 2.5-3 illustrates the G-189A components required to simulate the system for the 180 day life test reported in Reference 17.

$\text{CO}_2$  flow to the subsystem is supplied from  $\text{CO}_2$  accumulator component 1 (TANKG). The  $\text{CO}_2$  stored in this tank is assumed to have been collected by a  $\text{CO}_2$  concentration subsystem. The steam desorbed solid amines, hydrogen depolarized cell, or carbonation cell concepts are then potentially suitable for this purpose.  $\text{CO}_2$  flow is moved by component 2 (FAN) to humidifier component 3 (GASMIX). Here the  $\text{CO}_2$  is saturated with water prior to entering

the solid electrolyte cells. The saturated  $\text{CO}_2$  joins with recycle flow at component 4 (GASMIX) and then passes into the solid electrolyte cell component 5 (S $\ddot{\text{O}}$ LELC).

Component 5 represents several parallel modules of solid electrolyte cells. Each module is composed of a number of parallel stacks of electrolysis cells.  $\text{CO}_2$  is electrolytically decomposed into  $\text{O}_2$  and CO in the cells. Water also is electrolyzed into hydrogen and oxygen. Oxygen collected at the anode of the cells flows to oxygen accumulator tank component 6 (TANKG).

CO and  $\text{H}_2$  products and unreacted  $\text{CO}_2$  and  $\text{H}_2\text{O}$  reactants flow to hydrogen gas separator component 7 (MEMOD). Hydrogen is separated by selective diffusion through a semi-permeable membrane. Hydrogen separated in this component is moved by vacuum pump component 9 (VACPMP) to hydrogen accumulator component 9 (TANKG).

The primary side gas stream from the hydrogen separator flows to carbon deposition reactor component 10 (CARDP). Here CO is reconverted back into  $\text{CO}_2$  for cycling to the solid electrolyte cells. In a secondary reaction,  $\text{H}_2$  reacts with  $\text{CO}_2$  to form  $\text{H}_2\text{O}$  and CO. The effluent of this component is circulated by component 11 (FAN) back to combine with the subsystem  $\text{CO}_2$  feed gas.

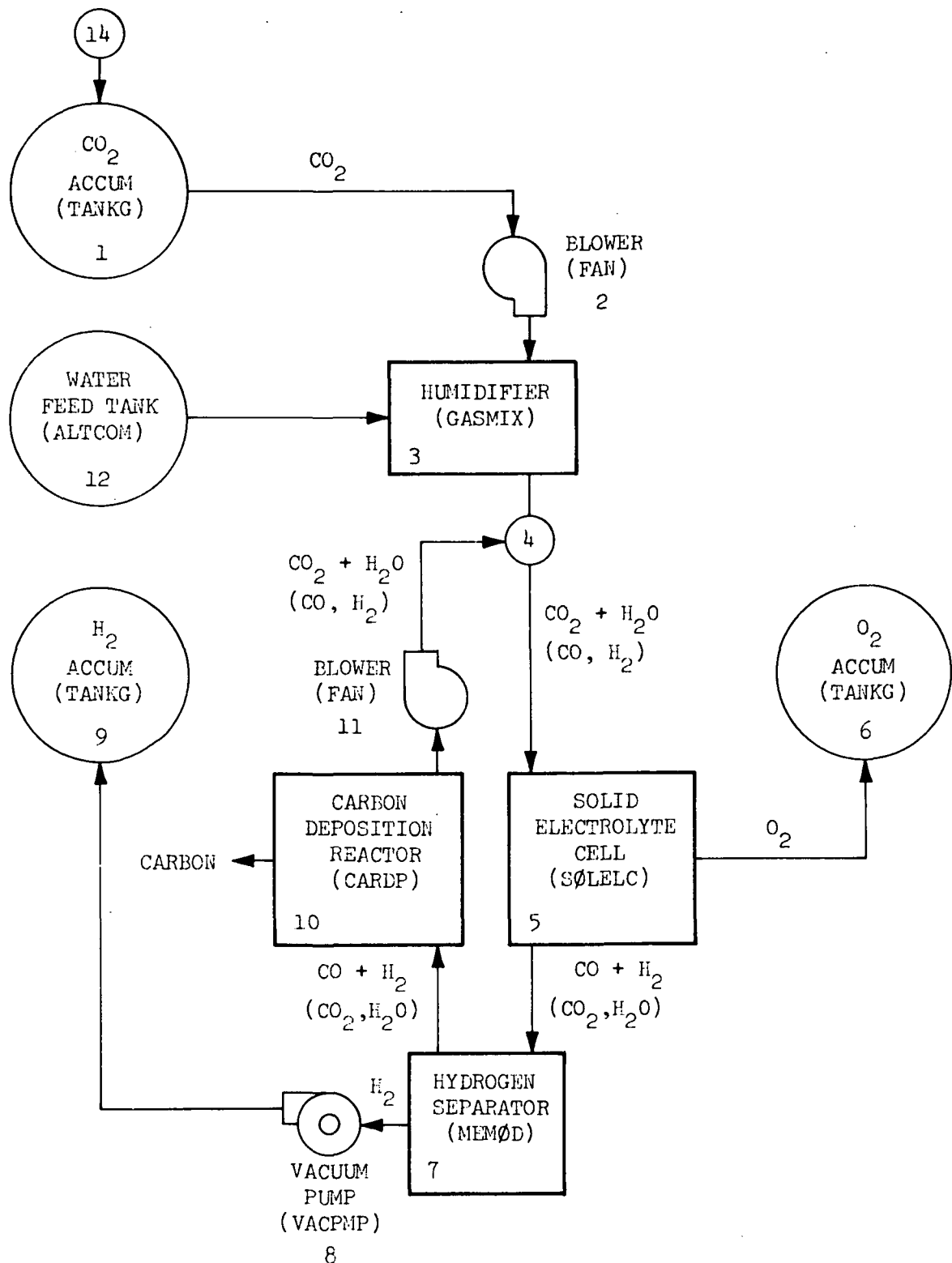
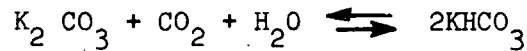


FIGURE 2.5-3 G189A SIMULATION OF SOLID ELECTROLYTE SUBSYSTEM

## 2.6 LIQUID ABSORPTION

### 2.6.1 Process Description

This process uses a liquid solution of potassium or sodium carbonate, or a mixture of both, to absorb  $\text{CO}_2$  from the cabin air. When carbon dioxide is absorbed in an aqueous solution of potassium carbonate, the following reversible reaction occurs:



Heating the bicarbonate solution and reducing the partial pressure of carbon dioxide in the gas stream causes bicarbonate to be reconverted to carbonate and  $\text{CO}_2$ .

The amount of carbon dioxide absorbed depends on several factors. These include the fraction of base that is bicarbonate, the normality of the base, and the partial pressure of carbon dioxide in the gas. The relationship between these variables at equilibrium conditions is given by the following equation (Reference 19).

for  $\text{K}_2\text{CO}_3/\text{KHCO}_3$

$$P_{\text{CO}_2} = \frac{45f_o^2 N^{1.29}}{S(1-f_o) (302-t)}$$

for  $\text{Na}_2\text{CO}_3/\text{NaHCO}_3$

$$P_{\text{CO}_2} = \frac{137f_o^2 N^{1.29}}{S(1-f_o) (365-t)}$$

where:

$P_{\text{CO}_2}$  = partial pressure of  $\text{CO}_2$  (mm Hg)

$N$  = normality of base ( $\frac{\text{g equivalents}}{\text{liter}}$ )

$S = \text{solubility of CO}_2 \text{ in H}_2\text{O at one atmosphere}$   $(\frac{\text{g moles CO}_2}{\text{liter H}_2\text{O}})$

$T = \text{temperature } (^{\circ}\text{F})$

$f_o = \text{fraction of total base that is bicarbonate}$

A schematic of a  $\text{CO}_2$  concentrator subsystem using the liquid absorption concept is shown in Figure 2.6-1.  $\text{CO}_2$  laden cabin air is introduced into a contactor where the air stream is mixed with an aqueous carbonate solution to promote absorption of  $\text{CO}_2$ . The absorption reaction is favored when the solution is approximately at room temperature. In industrial gas/liquid absorption processes, counter current flow is commonly used. However, it is difficult to envision a counter flow contactor for zero-g operation. Since a suitable zero-g design has not been yet defined, the contactor has been assumed to operate with co-current or parallel flow. A device for gas/liquid separation is located immediately downstream of the contactor to achieve separation of the cabin air stream from the carbonate solution.

A regenerative heat exchanger and external heat source is used to heat the carbonate solution prior to entering a liquid flash vaporizer. Here,  $\text{CO}_2$  is desorbed and a portion of the water in the solution is vaporized. The liquid and gas phases leaving the vaporizer are assumed to be in thermodynamic and chemical equilibrium. The liquid phase is recirculated back to the liquid contactor and the gas phase is pumped to a condenser/separator where  $\text{CO}_2$  is separated from water vapor. The  $\text{CO}_2$  is then transferred to a  $\text{CO}_2$  storage tank.

### 2.6.2 Simulation of Concept

A simulation model of the liquid absorption  $\text{CO}_2$  concentrator subsystem was prepared to facilitate evaluation of the concept and to define the subsystem's critical components and parameters such as solution flow, temperature, and pressures. Figure 2.6-2 shows the G-189A components

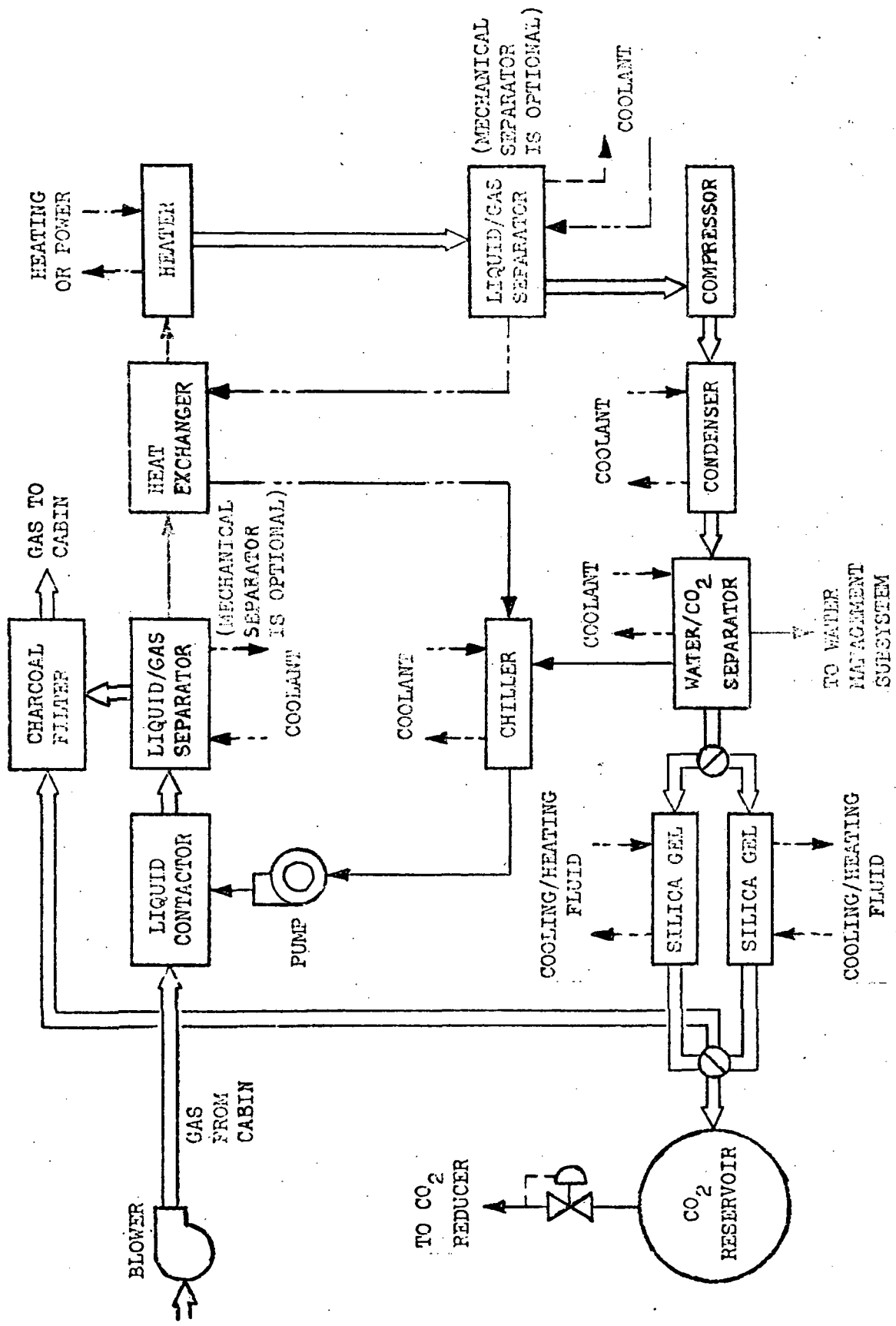


FIGURE 2.6-1 LIQUID ABSORPTION  $\text{CO}_2$  CONCENTRATOR

required for a typical subsystem. Inlet air, defined by component 1 (ALTCØM) is forced into the liquid contactor by blower component 2 simulated by subroutine FAN. The liquid contactor, component 3, is simulated by subroutine LIQCØN. This subroutine determines the amount of  $\text{CO}_2$  absorbed in a parallel flow contactor with the gas and liquid phases leaving in thermal and chemical equilibrium. The effluent from the contactor flows to component 4 (SPLIT) where the  $\text{CO}_2$  free cabin air is separated from the carbonate/bicarbonate solution. The air stream is dehumidified in component 5 (ANYHX) prior to being returned to the cabin.

The carbonate/bicarbonate solution flows through regenerative heat exchanger component 7 (ANYHX) and heater component 8 (ALTCØM) to raise the solution temperature to approximately 180°F. The solution then is partially vaporized in flash evaporator component 9 (LQFLSH).  $\text{CO}_2$  is desorbed into the gas phase as a result of the partial vaporization. The gas phase which evolves contains  $\text{CO}_2$  plus  $\text{H}_2\text{O}$  vapor. The liquid phase, which is in equilibrium with the gas phase, is a mixture of  $\text{H}_2\text{O}$ , carbonate, and bicarbonate.

The gas phase generated in the flash vaporizer is separated from the liquid phase and pumped by compressor component 16 (FAN) to condensing heat exchanger component 10 (ANYHX). Here,  $\text{H}_2\text{O}$  vapor is separated from the  $\text{CO}_2$ . The  $\text{CO}_2$  then flows to  $\text{CO}_2$  reservoir component 12 (TANKG). The liquid phase from the flash vaporizer (component 9) is recirculated by pump component 19 (PUMP) back through the regenerative heat exchanger (component 7). The solution then is chilled in heat exchanger component 15 (ANYHX) prior to returning to the liquid contactor (component 3).

Water vapor condensed and separated in components 5 and 10 is collected by component 13 (H2ØSUM) and transferred to storage tank component 14 (TANKG). Makeup water to the carbonate/bicarbonate loop is supplied by this component. This water enters the loop at component 17 (LIQMIX).

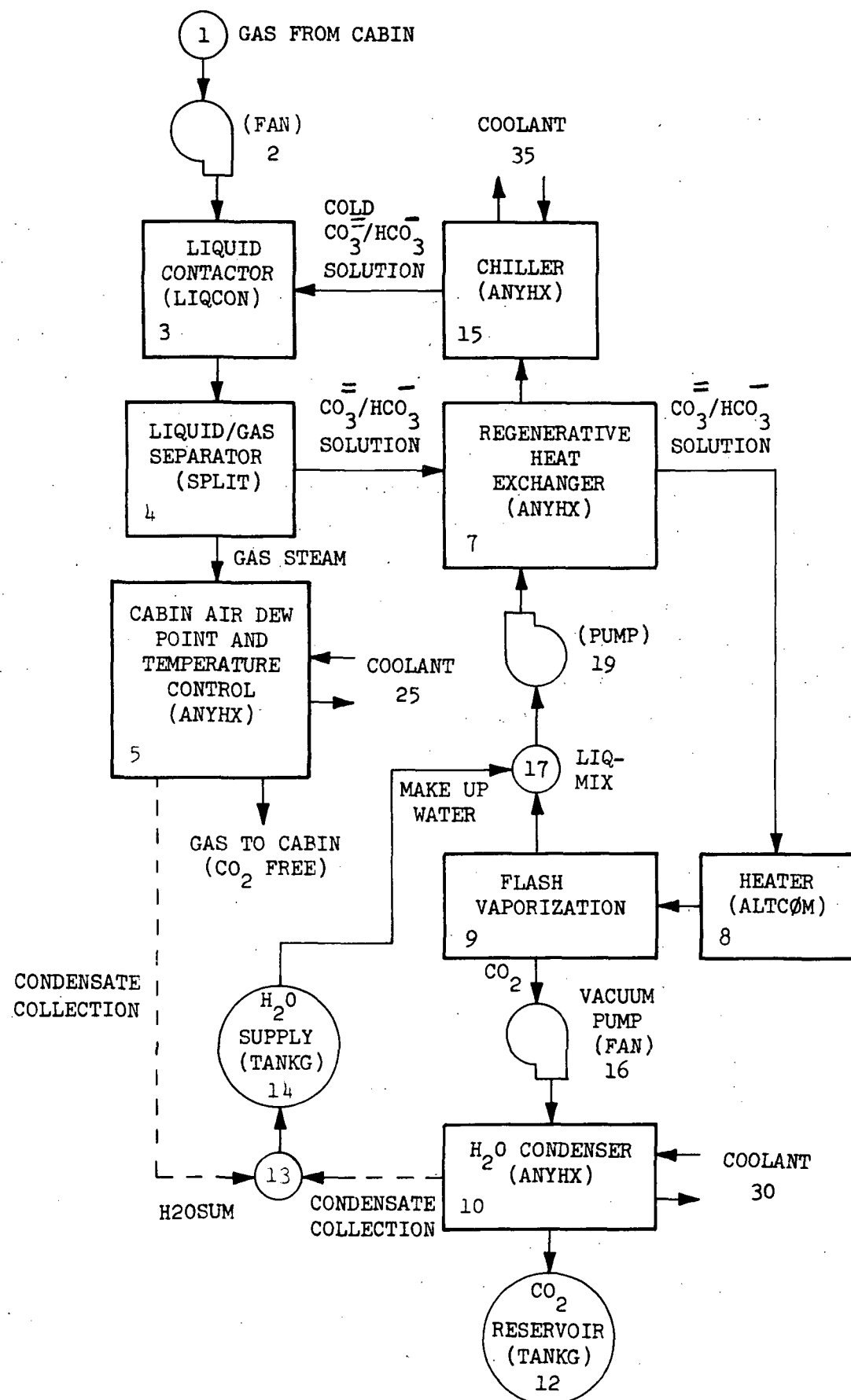


FIGURE 2.6-2 G-189A SIMULATION OF LIQUID ABSORPTION CO<sub>2</sub> CONCENTRATOR

## 2.7 ELECTRODIALYSIS

### 2.7.1 Process Description

A sketch of a typical Electrodialysis  $\text{CO}_2$  Management System is given in Figure 2.7-1. The most important components are the electrodialysis stacks since it is here that carbon dioxide is removed from air and oxygen is generated from water simultaneously. In general, cabin air is humidified and fed to absorber compartments where the carbon dioxide in the air is electrochemically converted to carbonate ions. Under the influence of an electrochemical potential, the carbonate ions are transferred out of the absorber into concentrator compartments where they react further to reform carbon dioxide gas. At the electrodes (anodes and cathodes) water is electrolyzed to form oxygen and hydrogen. Thus, if the system were treated as a black box, there are two inlet streams: water and cabin air containing carbon dioxide, and four effluent streams: oxygen, hydrogen, air with a reduced carbon dioxide content, and carbon dioxide (of greater than 99% purity). The basic principles involved in the electrochemical operations are electrodialysis and electrolysis. The description which follows was abstracted from References 20 and 21.

Electrodialysis is a process in which ionized molecules or atoms are transferred through highly selective ion-transfer membranes under the influence of a direct current. If a solution containing positively and negatively charged ions is fed to an electrodialysis cell, the positively charged ions (cations) will be attracted to the positively charged anode. The nature of the ion-transfer membrane between the solution and electrode (anode or cathode) determines whether or not an ion can migrate through it or be retained in the solution.

Anion-transfer membranes will allow anions to pass through them but exclude cations, while cation transfer membranes will allow the passage of cations but not anions. These membranes are highly selective for either anion or cation transfer. It is the selective properties of the anion and cation membranes which allow  $\text{CO}_2$  to be removed from the process air in one compartment

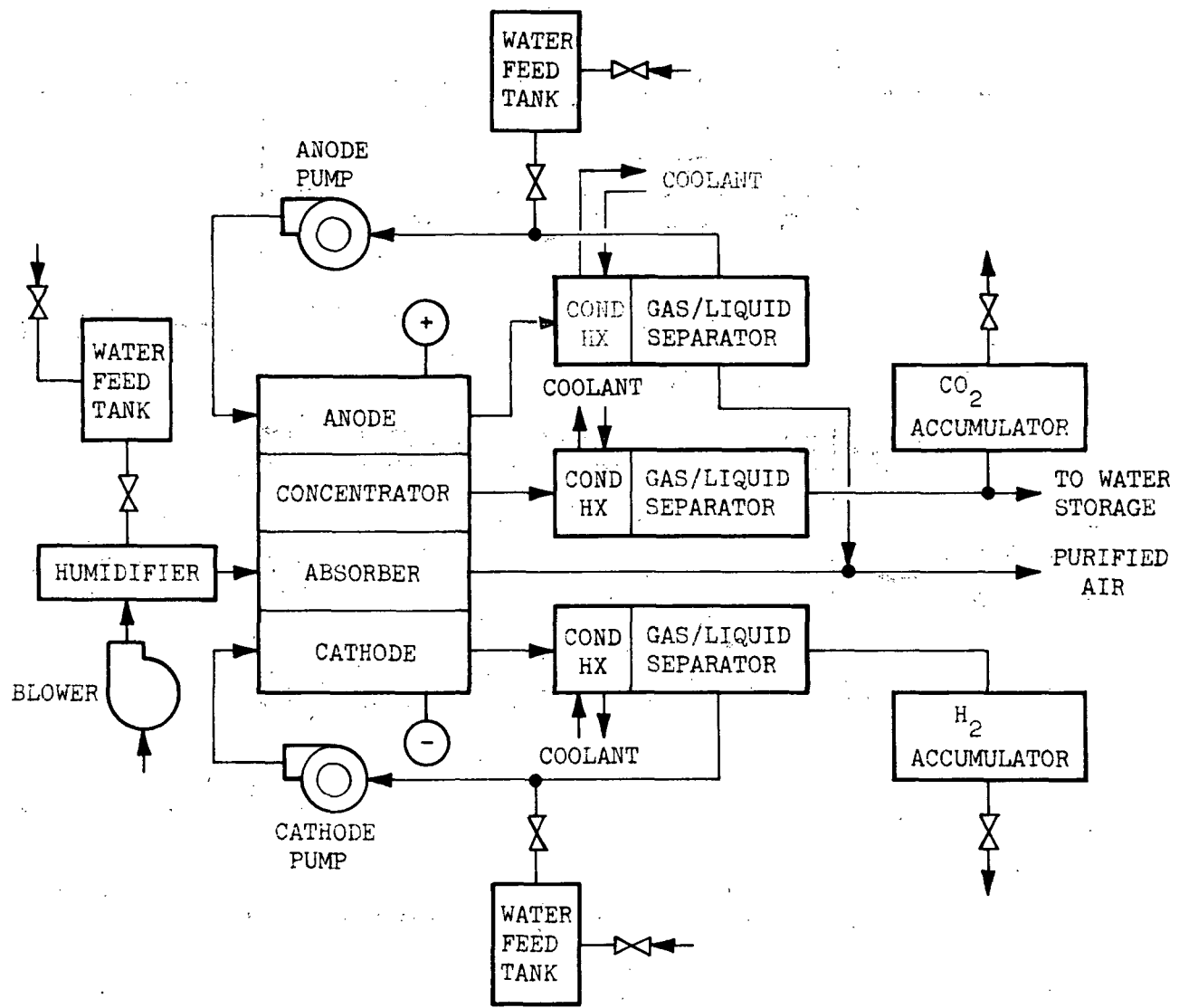


FIGURE 2.7-1 ELECTRODIALYSIS  $\text{CO}_2$  MANAGEMENT SYSTEM

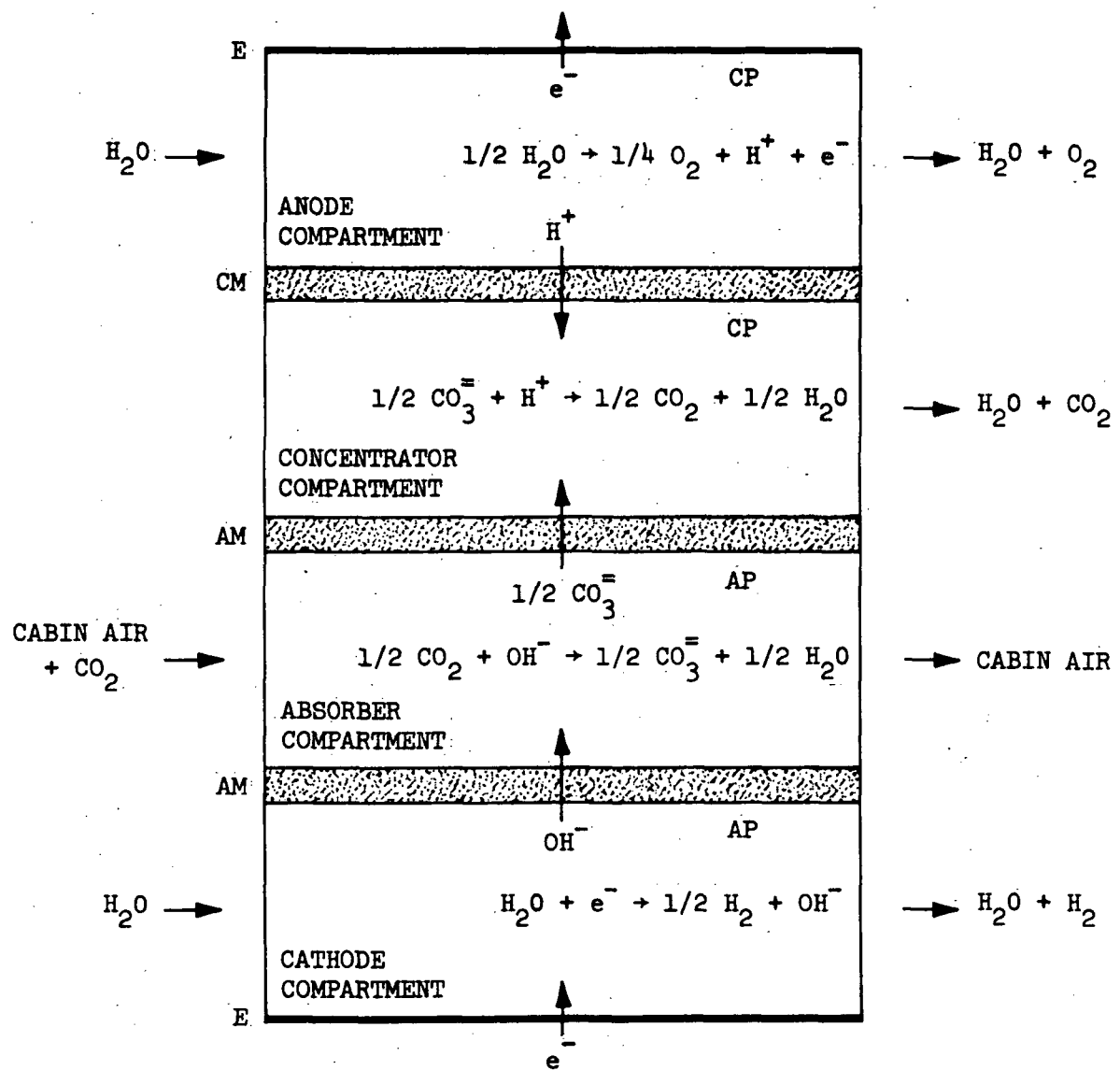


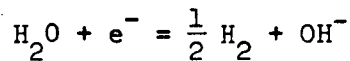
FIGURE 2.7-2 CARBON DIOXIDE ELECTRODIALYSIS CELL REACTIONS  
(SCHEMATIC OF BASIC REPEATING UNIT)

while  $\text{CO}_2$  is concentrated in an adjacent compartment. The two adjacent compartments are termed a cell pair. It is possible in this sort of arrangement to place as many as 500 cell pairs between a single pair of electrodes. The combination of cell pairs and electrodes is referred to as an electrodialysis stack.

The  $\text{CO}_2$  removal unit is comprised of repeating units consisting of four compartments: a carbon dioxide absorber, or scrubber; a concentrator compartment; an anode; and a cathode. The absorber and concentrator compartments can be termed a cell pair, while the anode and cathode compartments represent an electrode pair. The reactions which occur in the various compartments of this configuration are summarized in Figure 2.7-2.

The operation of the  $\text{CO}_2$  removal unit is as follows:

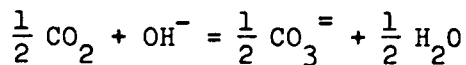
Liquid demineralized water is fed to the cathode compartment at a rate at least sufficient to provide for the water lost by electrolysis at the cathode,



and by electroendosmosis through the anion membrane into the absorber compartment. In any electrodialysis process as ions migrate across the membranes, water is transferred in the same direction. This water is apparently transferred due to the hydration of the ions as well as the electrical potential created by the movement of the ions through the pores of the membranes. The total water transfer is referred to as endosmotic water.

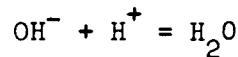
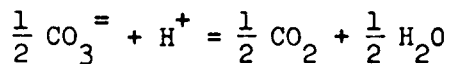
The liquid flow rate will be in excess of the electrochemical requirements to provide cooling of the stack and a sweep stream for the evolved hydrogen gas. A flow rate of about 8 gallons per hour is recommended in Reference 20 for a six-man unit at a cabin pressure of 7 psia.

Cabin air containing carbon dioxide is humidified and fed to the absorber compartment. In this compartment, which contains anion-exchange materials in the  $\text{OH}^-$  form, carbon dioxide is scrubbed from the air according to the following reaction,



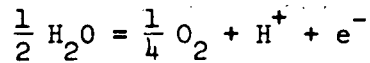
The anion-exchanger material is continually regenerated by the migration of hydroxyl ions from the cathode into the absorber compartment.

Carbonate ions, excess hydroxyl ions and endosmotic water are transferred from the absorber into the concentrator compartment which contains cation-exchange material in the  $\text{H}^+$  form. The following reactions occur:



The reformed carbon dioxide gas, along with the endosmotic water, passes out of the compartment under its own pressure.

Liquid (demineralized) water is fed to the anode compartment at a rate at least sufficient to provide for the water lost by electrolysis at the anode.



and by endosmosis through the cation membrane into the concentrator compartment. The water flow rate will be substantially in excess of the electrochemical requirements to aid in heat removal from the anode and to provide a sweep stream for the evolved oxygen gas. The hydrogen ions continually migrate into the concentrator compartment, where they serve to regenerate the cation-exchange material.

There is at least some liquid water present in all four streams effluent from the concentrator. This leads to a gravity-independent gas-liquid separation requirement which is readily provided (since no frothing or foaming has been observed) by small state-of-the-art, passive, gas-liquid separators having short holdup times.

The theoretical reactions shown in Figure 2.7-2 assume 100% carbonate ion transfer efficiency and electrode efficiencies. If 100% efficiencies are achieved in all operations in this type of stack,  $\text{CO}_2$  is absorbed in a 2:1 volumetric (or more) ratio to  $\text{O}_2$  production. The electrode reactions operate with about 100% efficiencies, while the membrane transfer process actually has efficiencies greater than 100% (under expected operating conditions).

This is explained by the formation of some monovalent bicarbonate ion ( $\text{HCO}_3^-$ ) in the absorber, which (for the same current flow) would transfer twice as much carbon dioxide as the divalent carbonate ion ( $\text{CO}_3^{=}$ ). Thus, the actual volumetric ratio of  $\text{CO}_2$  absorption to  $\text{O}_2$  production is greater than 2:1.

On the average a man expires 0.85 moles of carbon dioxide for every mole of oxygen inhaled (or a  $\text{CO}_2/\text{O}_2$  ratio of 0.85:1). If a membrane transfer efficiency of 120% is assumed for normal concentrator operation, then a  $\text{CO}_2/\text{O}_2$  ratio of 2.4:1 is attained. This means that this type of electro-dialysis stack does not supply sufficient metabolic oxygen while removing all the metabolic carbon dioxide. The remaining oxygen must be supplied by some other oxygen generation equipment.

It should be mentioned that experimental work has been conducted on electro-dialysis stacks containing only one anode and cathode compartment for a multiple number of absorber/concentrator cell pairs. An additional compartment or water cell is added to each absorber/concentrator cell pair to provide the necessary  $\text{H}^+$  and  $\text{OH}^-$ . By eliminating the anode/cathode compartments

with each cell pair, carbon dioxide can be removed from the atmosphere with almost negligible amounts of oxygen generated. However, the power requirements of these stacks have not been much lower than the power requirements of the Carbon Dioxide Scrubber described previously. In addition, between the cabin atmosphere leak rate and the metabolic loss of available oxygen (respiratory quotient of 0.85), there will be a significant oxygen supply requirement no matter what oxygen recovery subsystem is included in the space vehicle design.

### 2.7.2 Simulation of Concept

Figure 2.7-3 shows the G-189A components required to simulate a typical  $\text{CO}_2$  electrodialysis subsystem.

Cabin air is circulated through the concentrator by blower component 10 (FAN). The flow then passes through humidifier component 11 (GASMIX) prior to entering the electrodialysis cell module. Regulation of the humidity level in the process gas is necessary to prevent drying out of cell membranes.

Process gas flows into the absorption compartment of the electrodialysis cell component 12 (ELDIAL). Here,  $\text{CO}_2$  is removed by absorption and reaction with  $\text{OH}^-$  ions. The purified process gas then returns to the cabin or the humidity control subsystem (not shown). The  $\text{CO}_2$  removed in the absorption compartment migrates under influence of the cells' electrical field to the concentrator compartment. Here,  $\text{CO}_2$  is recovered in a "sweep fluid" provided by component 2. For this sample problem, water is assumed to be the "sweep fluid". The  $\text{CO}_2$  picked up by the sweep fluid is separated out in heat exchanger/water separator components 24 and 30 (ANYHX). The  $\text{CO}_2$  is compressed by 25 (FAN) and transferred to accumulator component 26 (TANKG).

The  $\text{OH}^-$  and  $\text{H}^+$  ions required for the chemical reactions occurring in the absorption and concentrator compartments, respectively, are supplied by water electrolysis reactions in the anode and cathode compartments. An alternate component, 13, is required for storing the outlet flow data for

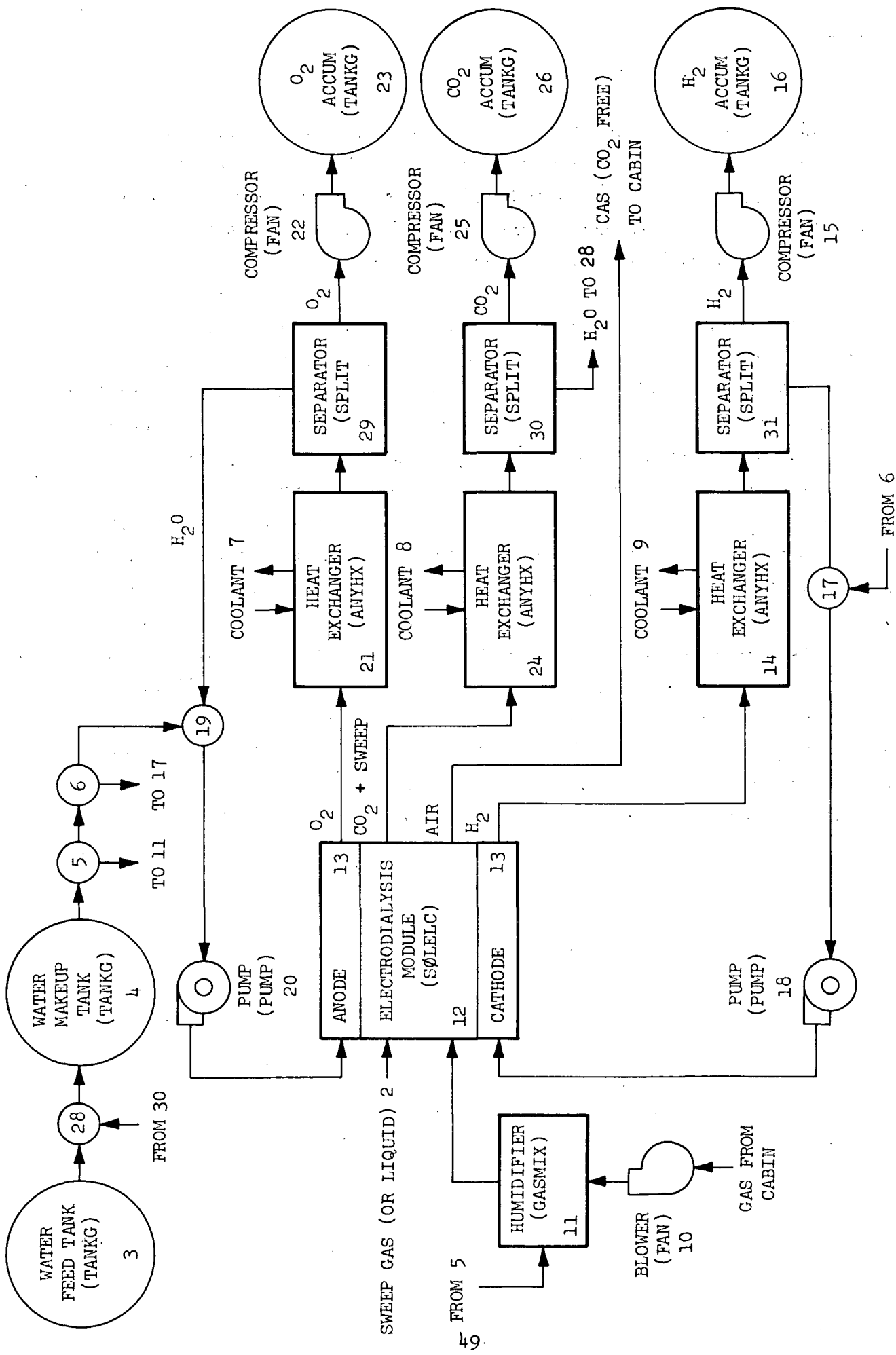


FIGURE 2.7-3 G189A SIMULATION OF ELECTRODIALYSIS CONCENTRATOR

the anode and cathode compartments. Liquid water is circulated to both of these compartments by semi-closed loops. Makeup water is compensated for electrolysis, chemical reaction, and electroendosmosis is provided to those loops by water makeup tank component 4 (TANKG). Flow to this tank is provided by water feed tank component 3 (TANKG).

Flow in the semi-closed cathode loop is circulated by pump component 18 (PUMP). Water entering the cathode compartment is electrolyzed to form  $H_2$  and  $\bar{OH}$  ions. The  $\bar{OH}$  ions migrate across a semi-permeable membrane into the absorber compartment. The effluent stream from the anode compartment flows to heat exchanger/water separator components 14 and 31 (ANYHX). Hydrogen separated from this stream is pumped by compressor component 15 (FAN) to accumulator component 16 (TANKG). The water separated is combined with makeup water at component 17 (LIQMIX) and recirculated. Cooling fluid to the condenser/water separator is provided by component 9.

The semi-closed water loop for the anode compartment is similar to that for the anode compartment. Water circulated by component 20 (PUMP) is electrolyzed to form  $O_2$  and  $H^+$  ions.  $O_2$  is separated from the anode effluent in heat exchanger/water separator components 21 and 29 (ANYHX). Makeup water enters the loop at component 19 (LIQMIX).  $O_2$  separated is transferred by component 22 (FAN) to  $O_2$  accumulator component 23 (TANKG).

## 2.8 MOLTEN CARBONATE

### 2.8.1 Process Description

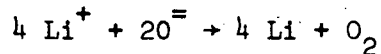
The molten carbonate process is an electrochemical process for reduction of  $\text{CO}_2$  absorbed from cabin air. In the basic concept lithium is reduced at the cathode of an electrochemical cell containing a molten lithium carbonate electrolyte. The lithium reacts chemically with carbon dioxide in solution to deposit solid carbon on the cathode surface and to form lithium and oxide ions in the electrolyte. At the anode, the oxide ions are oxidized to gaseous oxygen. Experimental work at Hamilton Standard Division of United Aircraft Corporation has indicated that the electrolysis of pure molten carbonate gives satisfactory results (Reference 22). However, its high melting point of  $735^\circ\text{C}$  ( $1,355^\circ\text{F}$ ), thus high operating temperatures, requires high temperature materials and associated high heat losses. These conditions also accelerate corrosion of the equipment. A lower melting point composition with similar conversion performance was found to be a eutectic mixture containing 60 percent by volume of lithium chloride and 40 percent  $\text{Li}_2\text{CO}_3$ . This eutectic mixture has a melting point of  $507^\circ\text{C}$  ( $943^\circ\text{F}$ ). The basic concept for the cell is illustrated in Figure 2.8-1.

The molten carbonate process, by accepting air directly from the cabin and reducing its  $\text{CO}_2$  to carbon and oxygen, does not require the  $\text{CO}_2$  concentration or water electrolysis units needed in other  $\text{CO}_2$  management concepts. One of the main design problems of this process concerns the phase separation between the gases and the molten salts, especially in null gravity conditions. Another problem is the removal of carbon deposited on the cathode. Molten carbonate units may use disposable cells that are discarded after a specified quantity of carbon has been deposited on the cathode (Reference 23). A porous matrix, made of sintered magnesium oxide, is used as the cathode. When wetted by the melt, a stable interface is formed in the matrix because of capillary surface tensions. The matrix should be dense enough to hold the electrolyte in place under all gravity conditions, yet sufficiently porous to allow ion mobility and an efficient

process. A screen (the anode) surrounds the electrolyte and the matrix. The anode screen and cathode matrix are held together by a metal diaphragm with deflects to accommodate the carbon deposited in the matrix.

### 2.8.2 Cell Details

Figure 2.8-1 is a schematic of a molten carbonate electrolyte cell. Electrolytic and chemical reactions at the electrodes are shown on the figure. The net electrolytic reaction is:



The theoretical cell voltage including  $\text{CO}_2$  partial pressure gradient effects is

$$E = 1.025 - \frac{RT}{4F} \ln \frac{P_{\text{CO}_2, c}}{(P_{\text{CO}_2, a}) (P_{\text{CO}_2}^0)^2}$$

This voltage applies to a cell where water vapor reactions have been eliminated by pre-drying the cabin air prior to entering the cell. Actual required cell voltage will be higher due to Joule heating losses and electrode overvoltage.

The required electrolysis current assuming 100% current efficiency is given by Faraday's law

$$I = 1100 \frac{\text{amp-hours}}{\text{lb CO}_2}$$

Other reactions will occur in the cell under certain conditions. The cathode region must be shielded to prevent  $\text{CO}_2$  from reacting with deposited carbon to form carbon monoxide (CO) since this gas is toxic if generated in significant amounts. Another possible side reaction is the hydrolysis of LiCl to form HCl. Experimental results indicate that this side reaction may be ignored.

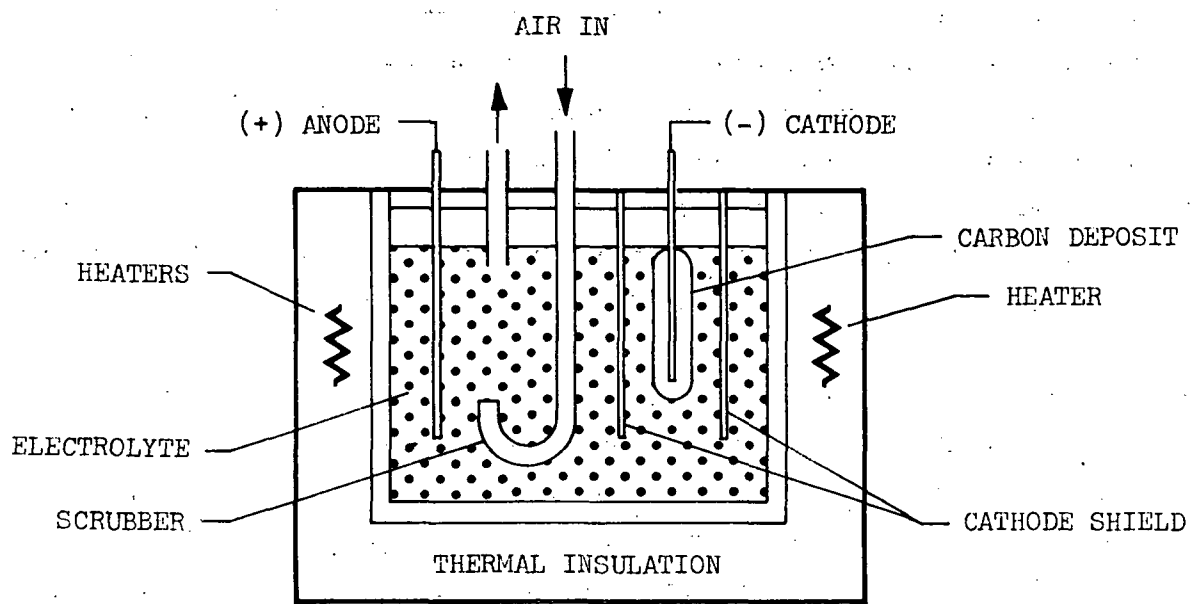


FIGURE 2.8-1 MOLTEN CARBONATE CELL

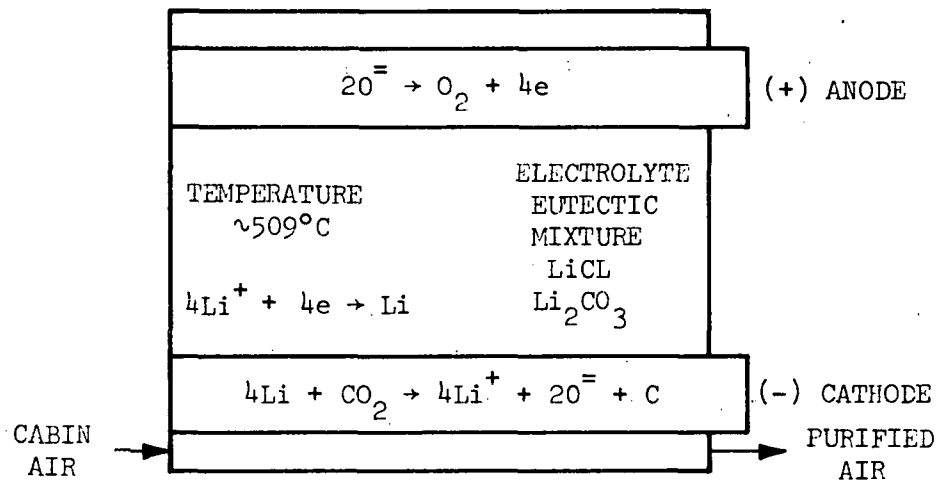


FIGURE 2.8-2 SCHEMATIC OF CELL REACTIONS FOR MOLTEN CARBONATE CELL

The level of water vapor in the gas feed can have a significant effect on cell reactions. For feeds with high water vapor pressure, the oxide ion ( $O^{=}$ ) concentration is inversely proportioned to the water vapor pressure. For a feed with little water vapor, the oxide ion concentration is inversely proportional to the carbon dioxide partial pressure. Since the main function of the cell is to decompose  $CO_2$ , water vapor partial pressure of the electrolyte must be made equal to the vapor in the process gas.

Water vapor pressure level also has an effect on cell voltage. At a given water vapor level, the potential between the cell electrodes will vary linearly with the logarithm of  $CO_2$  pressure ratio between the electrode. The slope of this relationship was found to change when the level of water vapor in the feed goes from a relatively small amount to a relatively high amount.

Methane and hydrogen contamination also have been detected at the cathode. These gases may form due to side reactions involving water vapor and the carbon deposited on the cathode. These reactions provide an additional reason for cathode shielding to prevent intermixing of these contaminant gases with the purified gas leaving the cell.

Contamination of oxygen generated at the anode with  $CO_2$  may occur if there is insufficient ionic diffusion to replenish oxide ions oxidized. Where ionic diffusion is insufficient chemical equilibrium will be shifted to generate  $CO_2$  and the required oxide ions form  $CO_3^{=}$ . This adverse reaction may be eliminated by limiting the current density to a value which allows sufficient ionic diffusion.

Several alternate compositions have been investigated for the melt (Reference 22). Melts using sodium, potassium or barrium salts in place of lithium, and lithium fluoride in place of lithium chloride are examples of alternatives studied. Generally, the alternatives yield inferior performance. However, the optimum melt composition probably is not defined at this time.

### 2.8.3 Simulation of Concept

Figure 2.8-3 illustrates the components and subroutines required for simulating a molten carbonate concept. The concept illustrated shows a silica gel bed for predrying the process gas. While elimination of water is not a requirement, some means is required to regulate inlet gas water vapor partial pressure to match the electrolyte water vapor pressure. A humidifier also could be used to achieve this control.

The cabin air process gas is circulated through the subsystem by blower component 2 (FAN). Air then flows to valve component 8 (SPLIT) where a portion is allowed to bypass the subsystem. Flow then passes through silica gel bed component 3 (ADSORB). Cooling fluid from component 12 is used to remove heat generated by absorption of water vapor. Component 3 and 7 operate in a cyclic fashion with one adsorbing while the other is desorbing. The source of liquid flow to these components changes as the components switch operating modes. After being dried in the silica gel bed, air flows to valve component 13 (SPLIT) which regulates the amount of air flowing to regenerative heat exchanger component 4 (ANYHX). The heat exchanger serves the dual function of preheating process air above the freezing point of the carbonate cell melt and of cooling outlet air sufficiently before return to the cabin.

Automatic controller component 10 (SERVO) is used to control cell temperature by regulating the amount of process gas bypassing the regenerative heat exchanger. Cell internal heat generation will vary with fluctuations in cell current and voltage. These fluctuations arise from regulation of cell operating conditions in response to cabin  $\text{CO}_2$  concentration. Another automatic controller, component 9 (SERVO), is used to control cell current. Since  $\text{CO}_2$  generation is a function of metabolic activity in the cabin, precise current control is necessary to match  $\text{CO}_2$  decomposition with the generative rate. Both controllers have "proportional position" controller action.

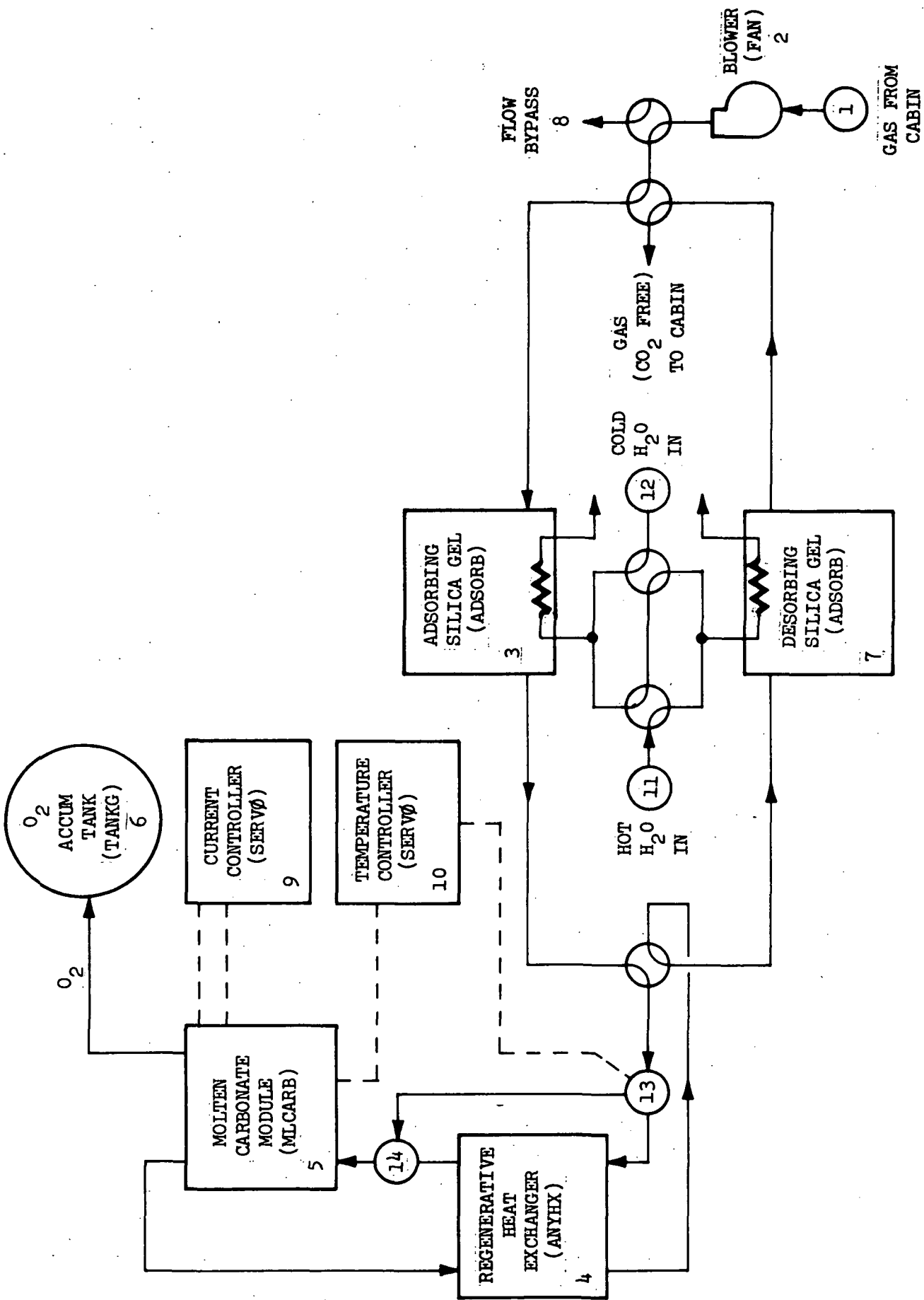


FIGURE 2.8-3 G189A SIMULATION OF MOLTEN CARBONATE CONCEPT

Process gas passes into molten carbonate component 5 (MLCARB) where absorption and reduction of  $\text{CO}_2$  occurs. The oxygen generated is collected in accumulator component 6 (TANKG) for use by the atmospheric supply subsystem. The purified process air passes back through regenerative heat exchanger component 4 to desorbing silica gel component 7 (ADSORB). Water vapor previously absorbed is driven off by heat supplied by heating fluid from component 12. Having been re-humidified, the purified air stream then returns back to the cabin.

## 2.9 MEMBRANE DIFFUSION

### 2.9.1 Process Description

Concentration by membrane permeation is a mass transfer process accomplished by a partial pressure difference and selective diffusion. The degree of separation is dependent on the difference in transfer rates of the component gases across the membrane. Membranes have been developed that yield a separation of 99% pure  $\text{CO}_2$ .

The membranes are packaged in multiple layers with intervening backing screens. The supply gas or "feed" gas is forced laterally through every other screen and "sweep" gas for removing outlet  $\text{CO}_2$  flow is forced through the alternate screens. The individual parallel passages for feed and sweep gas streams in the multiple layer configuration are manifolded together. Figure 2.9-1 from Reference 24 shows a representative multiple layer configuration. Figure 2.9-2 is a schematic representation of the design of a module.

Low pressure steam (15 mm Hg) is used as the sweep gas. The outlet  $\text{CO}_2$  is absorbed in the steam. The  $\text{CO}_2$  is removed from the water vapor in a condensing heat exchanger and it is subsequently pumped into an accumulator or is evacuated to space. The condensed water is revaporized for use as sweep gas.

The critical parameter is the permeability which has units of:

$$[\text{Perm}] = \frac{(\text{volumetric flow (STP)})}{(\text{time})(\text{area})} \frac{(\text{thickness})}{(\text{CO}_2 \text{ pressure differential})}$$

Increasing the  $\text{CO}_2$  pressure differential reduces the mass transfer area and this, in turn, directly reduces the weight and volume of the packaged module. In Reference 24 the  $\text{CO}_2$  inlet pressure was increased from 7.6 mm Hg to 35.8 mm Hg through compressing the feed flow total pressure from 258 to 760 mm Hg. This procedure is feasible when the cabin pressure is much

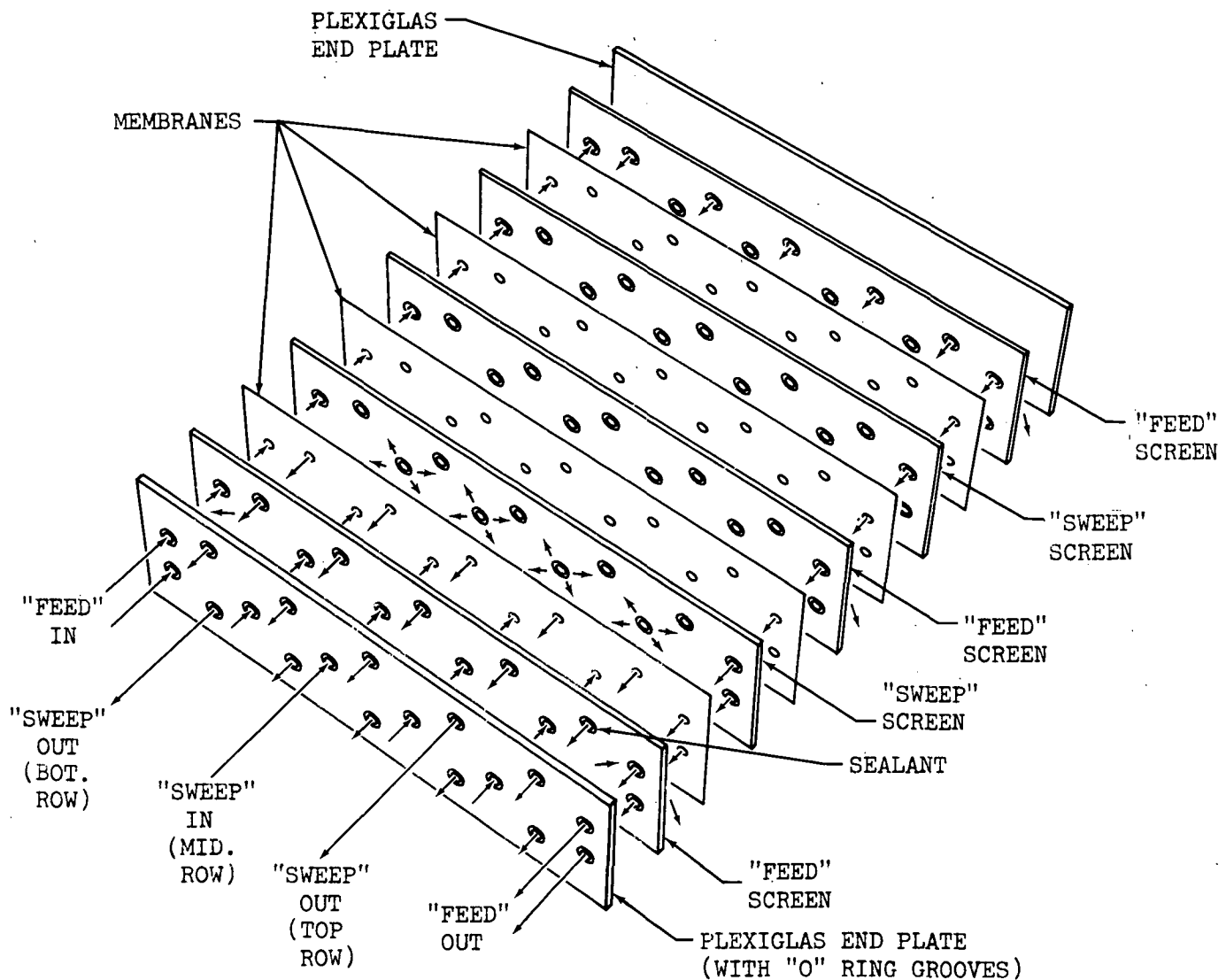


FIGURE 2.9-1 MEMBRANE MODULE

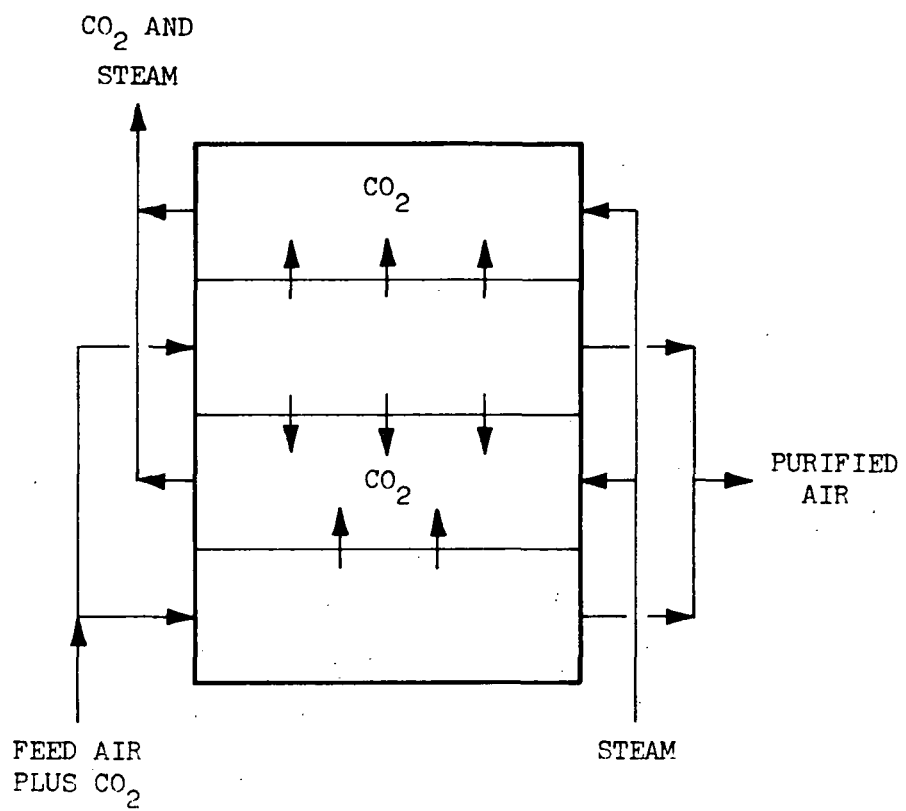


FIGURE 2.9-2 MEMBRANE DIFFUSION MODULE

less than 1 atmosphere. The membranes tested in Reference 24 were subjected to pressure differentials of 1 atmosphere or less. Some difficulties in maintaining satisfactory seals, preventing pinholes leaks, and preventing scoring of membranes by the backing screens were experienced at pressure differentials of 1 atmosphere. The bubble point for the membranes was over 30 psi so 15 psi pressure differential was considered to be safely below the maximum allowable pressure differential. When cabin pressures are high the  $\text{CO}_2$  pressure could again be increased by compressing the feed gas providing a membrane can be developed which would successfully withstand the resulting pressure differential. This technique would require that the membrane module be constructed as a pressure vessel. Preliminary calculations have indicated that for total pressures up to 10 atmospheres the weight of the pressure shell is only of the order of 10% of the basic membrane module.

#### 2.9.2 Membrane Description and Cell Details

The degree of separation ( $\text{CO}_2$  removal) is dependent on the difference of transfer rates and pressure differential of the constituent gases across the membrane. The rate controlling mechanism is a flow conduction process involving the adsorption and solution of a constituent, diffusion of solute through the barrier under a concentration potential (pressure differential), and desorption and evaporation of solute from the surface. One well known membrane is silicone rubber which combines high  $\text{CO}_2$  permeability and high  $\text{CO}_2/\text{O}_2$  separation factor (ratio of  $\text{CO}_2$  permeability to  $\text{O}_2$  permeability) of 5.5. However, for a practical  $\text{CO}_2$  removal system, this separation factor is inadequate.

Highly effective, immobilized liquid membranes that yield a  $\text{CO}_2/\text{O}_2$  separation of 99 + % were developed. Initially, an immobilized liquid film was made by containing a 1 to 2 mil porous Dacron mat impregnated with saturated  $\text{CsHCO}_3$  solution backed by silicone rubber membranes. However, it was found that the caustic  $\text{CsHCO}_3$  solution attacked the silicone rubber causing pinholes

to develop, resulting in cross-membrane leaks and a low separation factor. In place of the rubber membrane, a microporous, hydrophobic film manufactured under a trade name "Solvineert" by Millipore Corporation was found to be effective in providing a method for immobilizing the liquid film. The Solvineert film is unaffected by the aqueous salt solutions used and the bubble point of liquid impregnated silicon (the presence required to blow the liquid through the pores of the film) was in excess of 30 psi.

Since the membrane consists of saturated  $\text{CsHCO}_3$  solution backed by the Solvineert filters, it is desirable to operate the sweep side of the package with a water vapor sweep stream at a total pressure equal to the equilibrium vapor pressure of the aqueous solution. This enables recovery and reuse of both constituents of  $\text{CO}_2\text{-H}_2\text{O}$  sweep stream, a necessity for long term missions. In addition, the air at the feed side should be water saturated to prevent the drying of the feed side of the membrane and pinhole leaks developing.

A  $\text{CO}_2$  scrubber using the Solvineert membranes with a projected packaging density of  $440 \text{ Ft}^2/\text{Ft}^3$  was developed for the Air Force Flight Dynamics Laboratory. The membranes were packaged in multiple layers with intervening backing screens. The supply gas or "feed" gas is forced laterally every other screen (Figure 2.9-1). A summary of membrane and screen details is given below:

Membranes:

Millipore Corporation "Solvineert" films  
Microporous, hydrophobic film, pore size  $20\mu$   
porosity 70%, thickness .005 in, impregnated  
with aqueous  $\text{CsHCO}_3/\text{NaAsO}_2$  solution:

$6.4 \text{ M CsHCO}_3$ , 99.9% pure

$.25 \text{ M NaAsO}_2$

1% to 2% by volume polyethylene glycol

Feed Gas Screens: PE 400 polyester monofilament screens, thickness .013 in., 400 mesh openings, 47% open area

Sweep Gas Screens: PE 1120 polyester monofilament screens, thickness .024 in., 120 mesh openings, 58% open area

### 2.9.3 Simulation of Concept:

The G-189 simulation of the  $\text{CO}_2$  removal system using the membrane diffusion concept is shown schematically in Figure 2.9-3. Inlet air, defined by a dummy component (component 1) is forced to a condensing heat exchanger for humidity control (component 3) by a high pressure fan simulated by subroutine FAN, component 2, simulating a compressor. As the air passes through the membrane module (component 4), a portion of the  $\text{CO}_2$  permeates the membrane to the "sweep" side of the module which is using steam as the sweep gas. The purified air is returned to the cabin. The  $\text{CO}_2$  that permeates through the membranes is pumped along with the sweeping water vapor stream to a condenser-separator, component 6, for  $\text{H}_2\text{O}/\text{CO}_2$  separation. The  $\text{CO}_2$  is then pumped by component 7, simulated by PUMP, to the  $\text{CO}_2$  accumulator which is simulated by subroutine TANKG, component 8.

The condensed water from both condensing heat exchangers, components 3 and 6, is removed and summed by the new subroutine, H20SUM, "The Water Summation Subroutine". This subroutine sums condensate flow from up to 5 condensing heat exchangers and determines the mix temperature of total flow.

A method for adding makeup water for this  $\text{CO}_2$  removal system is provided by component 10, LIQMIX, by providing for  $\text{H}_2\text{O}$  flow from the water supply subsystem. The makeup water from water supply will be added as required, to the  $\text{H}_2\text{O}$  accumulator, component 11, to maintain a relatively constant  $\text{H}_2\text{O}$  level in the  $\text{H}_2\text{O}$  accumulator. The required rate of addition will be determined by GPOLY logic. Component 12, simulating an  $\text{H}_2\text{O}$  pump, provides constant water flow from the accumulator to the steam generator, component 13.

The steam generator is simulated by a new subroutine SMGEN. SMGEN is used to supply superheated steam for use in various EC/LS subsystems such as the CO<sub>2</sub> removal system utilizing the membrane module.

A new subroutine was written to simulate component 4, membrane module. This new subroutine, MEMOD, models the mass and thermal balance of a membrane module which would have gases of different concentrations flowing through the modules two sides.

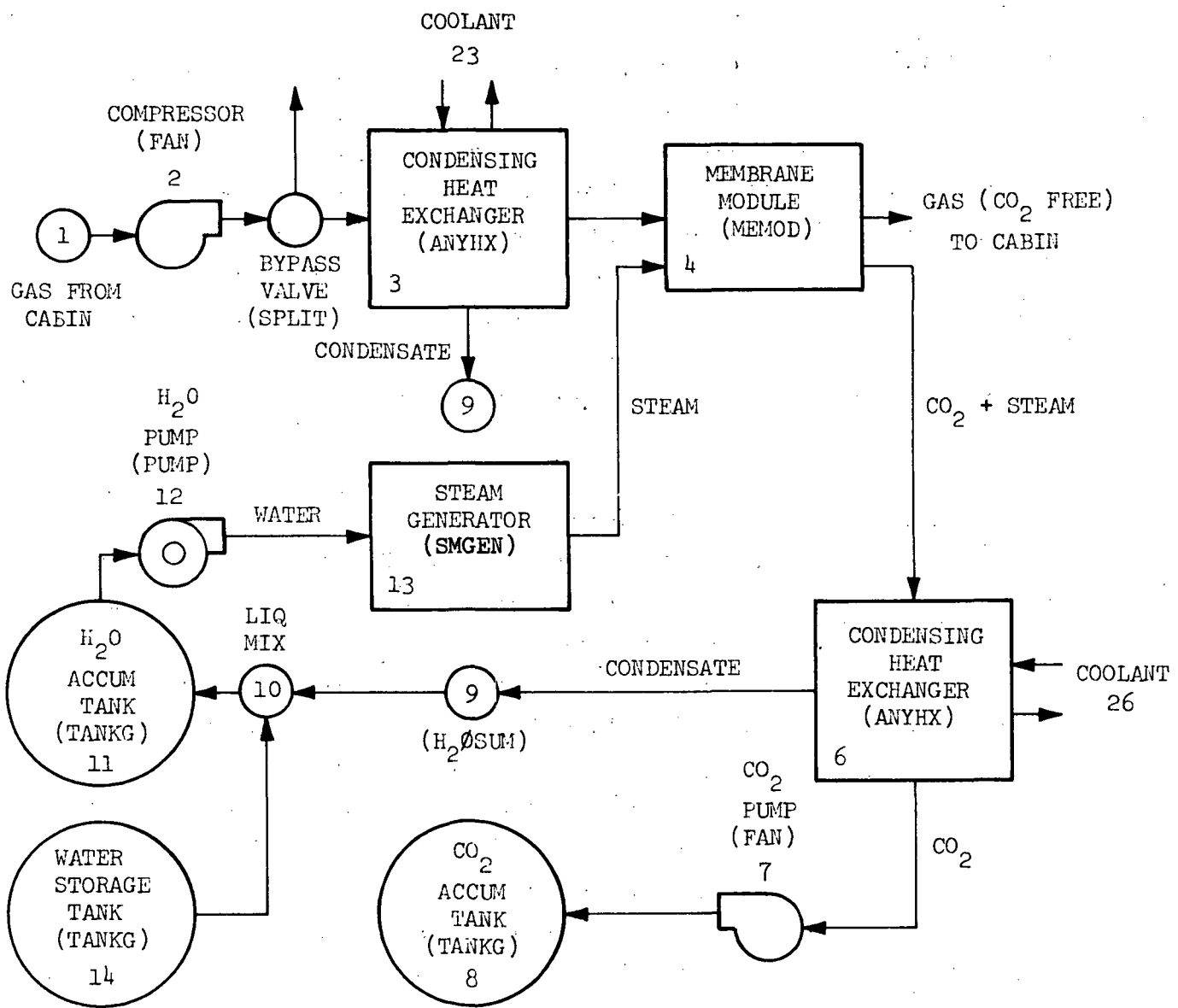


FIGURE 2.9-3 G189A SIMULATION OF MEMBRANE DIFFUSION CONCEPT

## 2.10 MECHANICAL FREEZOUT

### 2.10.1 Process Description

In this process  $\text{CO}_2$  is removed from cabin air by precipitation in suitably designed channels of a heat exchanger device. The precipitation occurs when the temperature of the gas is sufficiently lowered through heat exchange to a refrigerant or low temperature sink. In the range of  $\text{CO}_2$  partial pressures encountered, carbon dioxide begins to precipitate at  $-125^\circ\text{C}$  ( $\text{PPCO}_2 = 5.0 \text{ mm Hg}$ , saturated) and its removal will practically be total at  $-140^\circ\text{C}$  ( $\text{PPCO}_2 = 0.43 \text{ mm Hg}$ , sat.). Water is assumed to be completely removed using the silica gel bed upstream of the precipitation channel and will not interfere with either the precipitation or sublimation of the carbon dioxide.

Several carbon dioxide removal system utilizing the freezout concept have been proposed; however, only the two more practicable systems will be presented here. The first system, shown in Figure 2.10-1, uses precipitator/sublimator coupled to a very cold space radiator to remove the  $\text{CO}_2$ ; the second system, shown in Figure 2.10-2, requires the use of a refrigeration system. The space radiator and the refrigeration system are necessary in both cases for thermal energy removal to account for the inefficiencies of the regenerative heat exchangers that are being utilized and the heat flux from the surroundings into the system. Both systems use a water condenser for humidity control, and a silica gel bed for predrying the cabin air before passing it through the regenerative heat exchanger. It is imperative that the air be dried prior to its passage into the regenerative heat exchanger to prevent the buildup of frost which would deteriorate its performance.

The  $\text{CO}_2$  removal system which utilizes the precipitator sublimator, hereby referred to as the P/S system, will be considered to be an open system. Its operation predicates the simultaneous precipitation and sublimation of  $\text{CO}_2$  frost. For sublimation to occur, the  $\text{CO}_2$  frost must be exposed to the

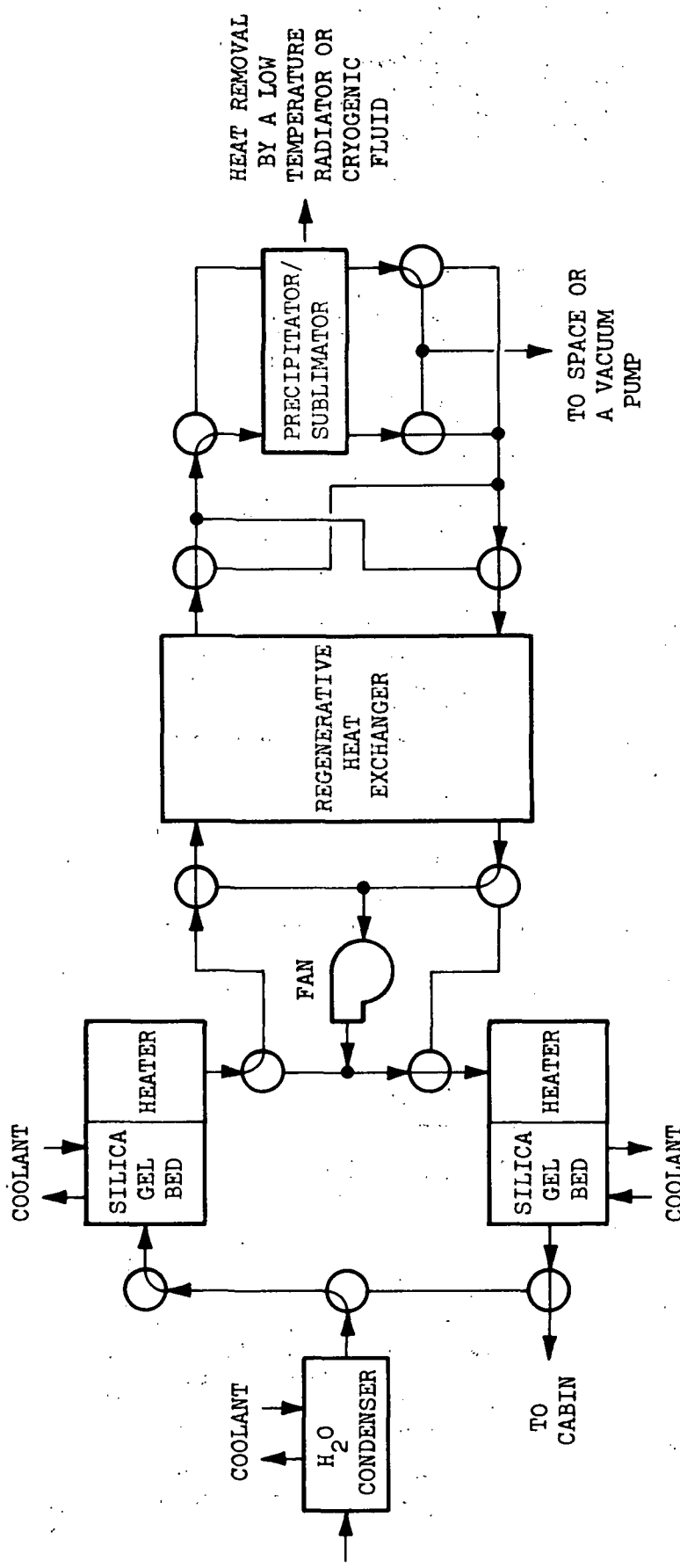


FIGURE 2.10-1 MECHANICAL FREEZE-OUT SYSTEM, NON-RECOVERABLE CO<sub>2</sub>

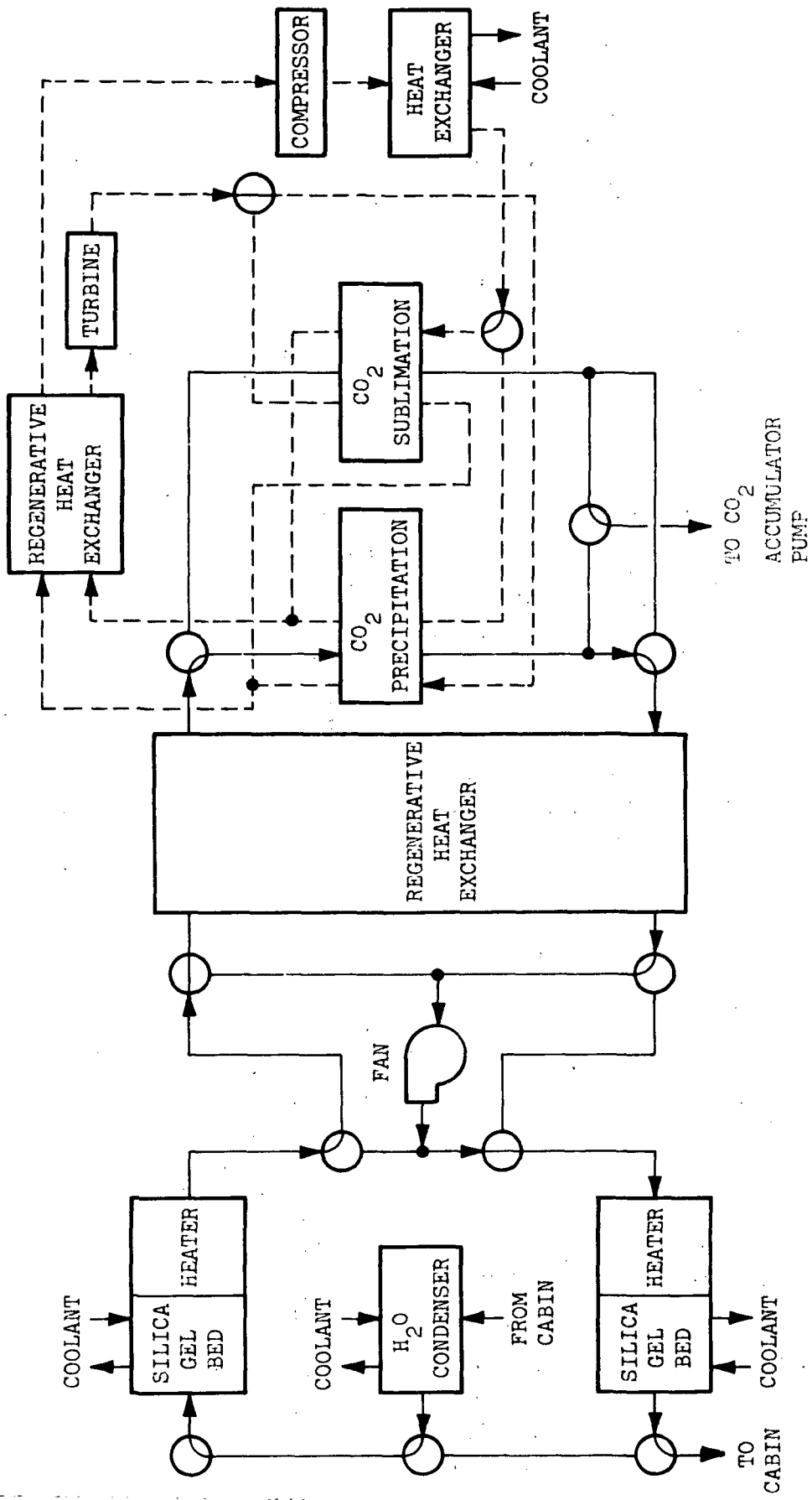


FIGURE 2.10-2 MECHANICAL FREEZE-OUT SYSTEM, RECOVERABLE  $\text{CO}_2$

vacuum of space. In the simultaneous precipitation and sublimation, the heat of precipitation supplies the thermal energy required for the sublimation to space. However, to account for the inefficiency of the regenerative heat exchangers and the heat influx into the  $\text{CO}_2$  removal system due to pipe connectors and supports, a method for removal of thermal energy must be included. Two methods for the removal of thermal energy have been proposed. The first method described in Reference 25 and 26 uses cryogenic  $\text{O}_2$ ,  $\text{N}_2$  or  $\text{H}_2$  to remove the heat to make the system operational. The second method employs a low temperature radiator to reject the heat from system to drive the precipitation sublimation process. This method, described in References 27, 28, and 25, relies on the ability to design a radiator that operates at  $-250^{\circ}\text{F}$  which presently does not appear feasible.

The Mechanical Freezout System-Recoverable  $\text{CO}_2$ , shown in Figure 2.10-2, uses a refrigerant to chill the cabin air flowing through the precipitation channel. This type of system minimizes the total vehicle weight penalty at the expense of an increase in required power input. For long-duration space missions, studies have shown (Reference 26) that the reversed Brayton-cycle system offers the most desirable method for heat removal. The reversed Brayton cycle system offers the following advantages with respect to the other systems:

Employs a single phase fluid and thereby its operation is simpler and more flexible than the Claude cycle.

The entire expansion occurs in a turbine, thus allowing high temperature operation which is more efficient.

In addition, the system has potential for long-duration maintenance-free operation.

The use of the hotter compressed gas in the refrigerant system to sublime the  $\text{CO}_2$ , as shown in Figure 2.10-2, affords a method for the recovery of the precipitated  $\text{CO}_2$  without the use of deep space vacuum (thermal sublimation). In addition, more positive control of the precipitation and submimation processes is provided.

### 2.10.2 Simulation of Concept

The simulation of the mechanical freezout concept is performed by dividing the subsystem into major functional components which may be mathematically modeled by G-189A component subroutines.

Figure 2.10-3 shows the G-189 component connection and definition diagram which was prepared for the analysis of the subsystem. Dummy component 1 (subroutine ALTCOM) is used to define the inlet conditions (flowrate, temperature, humidity,  $\text{CO}_2$  partial pressure, constituency, etc.) to the subsystem.

A  $\text{H}_2\text{O}$  condenser, component 2 (ANYHX), is used in conjunction with a silica gel bed, component 3 (ADSØRB), to dry the air sufficiently to prevent  $\text{H}_2\text{O}$  freezout in the  $\text{CO}_2$  precipitating heat exchanger, component 6. Dummy component 12 (ALTCOM) provides the coolant to the condensing heat exchanger at a specified temperature and flowrate. The condensate is pumped by component 17 (PUMP) to a water storage tank, simulated by component 18 (TANKG).

The dehumidified air from the silica gel bed passes through a switched off heater, component 4 (ALTCOM), to regenerative heat exchanger, component 5 (ANYHX). Here the air is pre-cooled prior to entering the  $\text{CO}_2$  precipitator. The secondary flow for this component is the effluent from the precipitator heat exchanger.

The precipitator heat exchanger, component 6, is simulated by a modified version of subroutine ANYHX. A new subroutine, CO2CP, has been added to the program to simulate the  $\text{CO}_2$  precipitation process in the heat exchanger component. In addition to determining the amount of precipitation, this subroutine determines the effective specific heat of the process air entering and leaving the precipitator. Refrigerant flow to the precipitator is supplied by dummy component 16 (ALTCOM).

Air flow from the precipitator is circulated by fan component 7 (FAN) back through the regenerative heat exchanger to heater component 8 (ALTCØM) and desorbing silica gel bed component 9 (ADSØRB). The heater component provides the thermal energy required to force water vapor desorption in the silica gel bed.

The sublimation of  $\text{CO}_2$  is simulated with component 10 (ANYHX). The rate of sublimation is assumed to equal the rate of precipitation in component 6. This rate, which is the difference between the flow of  $\text{CO}_2$  in and out of the precipitator, is calculated by GPØLY logic. Dummy component 19 is used to supply  $\text{CO}_2$  to the sublimator at a rate equal to the sublimation rate of the solid  $\text{CO}_2$ . This energy is removed from heating fluid circulating through the sublimator. The heating fluid, which is assumed to be gaseous nitrogen is supplied by component 11. The  $\text{CO}_2$  sublimated is pumped by component 14 (PUMP) to  $\text{CO}_2$  accumulator component 15 (TANKG).

Because of the cyclic operation of the system, components 3 and 9, 4 and 8, and 6 and 10 alternately switch functions according to a pre-determined time sequence. Logic is incorporated in GPØLY to change the order of solution path, modify sources of flows, and perform other miscellaneous operations when the switch of functions occurs.

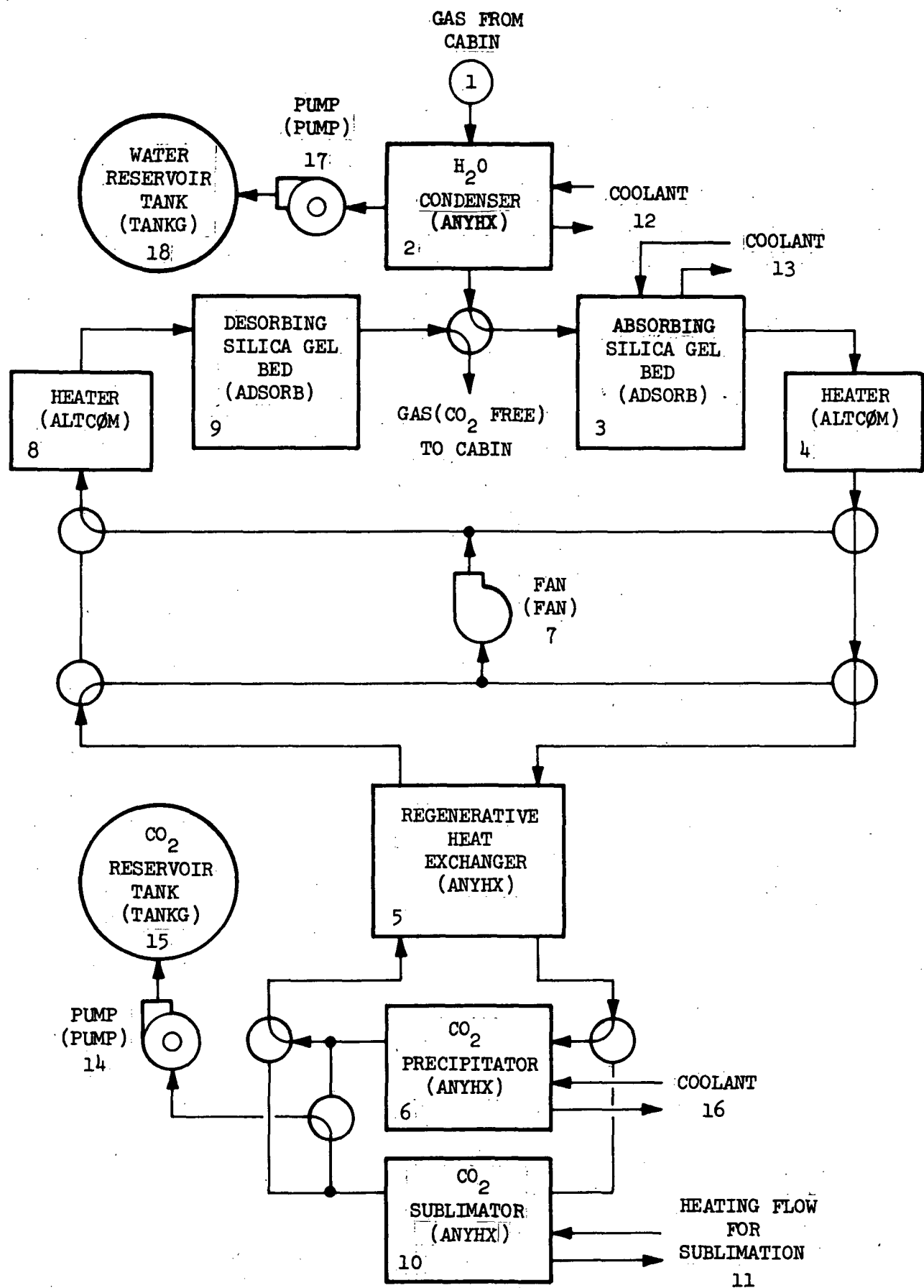


FIGURE 2.10-3 G189A SIMULATION OF MECHANICAL FREEZE-OUT

### 3.0 CONCLUSIONS AND RECOMMENDATIONS

The subroutines prepared should provide adequate representations of the overall mass and energy balances for the parametric performance of the concepts considered. In preparing the subroutines several areas where additional effort may be warranted are as follows:

- o Determining parametric scaling laws for weight, volume, and power for the ten concepts.
- o Performing laboratory testing of the concepts to fully define subsystem parameters or physical properties.
- o Performing system integration studies for the concepts when coupled with various oxygen regeneration subsystems or complete EC/LS systems.
- o Determining the optimum concept by evaluating the parametric performance of each concept for a wide range of mission, environmental, or operating conditions.
- o Performing reliability and cost analysis studies for the ten concept.

The above recommendations cover a wide gambit of effort. It is probable that some of the concepts may be eliminated from further consideration and that the major emphasis should be placed on perhaps 4 or 5 of the concepts.

In selecting the optimum subsystem, certain other intangibles must be considered. For instance, the year in which space type hardware could be expected to be available. Problems with contamination, corrosion, impacts on the cabin thermal environment, and safety must be assessed. Also the subsystems compatibility with the spacecraft power system.

In general it can be stated that concurrently with laboratory testing of the concepts, the computer subroutines should be used to model the test conditions. In addition to providing a test of the adequacy of the computer math models, this will allow a better understanding of the test results. It can also be stated that having defined those system parameters which are important to the mathematical models, additional laboratory testing is necessary to verify the values of these parameters. Several specific areas where improvements could be made in the simulation models are presented in the following subsections.

### 3.1 Steam Desorbed Resins

Additional laboratory testing is necessary to determine  $\text{CO}_2$  and  $\text{H}_2\text{O}$  equilibrium data at temperatures between 180-220°F. This is the temperature range in which  $\text{CO}_2$  is desorbed by steam stripping. The data is required since the rate of mass transfer from the bed to gas is equal to the mass transfer coefficient times the difference between the gas phase partial pressure and the equilibrium partial pressure correspondingg to the sorbate bed loading.  $\text{CO}_2$  equilibrium data is required for  $\text{CO}_2$  bed loadings from 0 to 3.5% and  $\text{H}_2\text{O}$  bed loadings from 0 to 40%.  $\text{H}_2\text{O}$  equilibrium data, which is assumed to be independent of  $\text{CO}_2$  loading, is required for  $\text{H}_2\text{O}$  bed loadings from 0 to 40%. An empirical correlation for overall mass transfer coefficient as a function of operating conditions is also required. Parametric computer runs then should be made to compare subroutine results with test data. The relative importance of interparticle diffusion needs to be assessed. More important, the mechanism for mass transfer should be carefully re-evaluated. Can the mass transfer rate be predicted strictly from the equilibrium data and mass transfer coefficient, or are the effects of chemical reaction kinetics more important? Should the water vapor transfer be calculated on a stoichiometric basis from the amount of  $\text{CO}_2$  desorbed?

Additional testing may be warranted to verify the heats of sorption for  $\text{CO}_2$  and  $\text{H}_2\text{O}$  on the resin particles. Physical properties for the particles, such as bulk density, void fraction, superficial surface area, specific

heat, etc., must be carefully defined. Additional testing also is required for determining the heat transfer characteristics of the bed. In particular, the effective thermal conductivity of the resin material is required. If the bed contains an integral heat exchanger, the overall thermal conductivity between the heat exchanger/gas or heat exchanger/pellets should be evaluated.

### 3.2 Vacuum Desorbed Resins

At the present time no equilibrium data is available for Gaf-O-Sorb resin which is considered the most promising resin for this concept. Equilibrium data is required for approximately the same set of temperature and bed loadings as for the steam desorbed concept. Data on the physical properties of the resin such as bulk density, superficial surface area, void fraction, etc., also are lacking.

The same general comment made for the steam desorbed resin which called for additional analysis of the mechanism for mass transfer also applies. Additional data also is required for mass transfer coefficients, heat of sorption, and heat transfer characteristics. Since, for this concept, the bed contains an integral heat exchanger, the importance of a careful definition of the heat transfer characteristics should be emphasized.

### 3.3 Carbonation Cell

The math models for the subroutines used in simulating this concept are relatively unsophisticated. However, additional complexity is most likely not warranted since the concept is generally considered to have been superseded by the hydrogen depolarized cell. Assuming the math models to be adequate, a better definition of cell design characteristics is required for an adequate simulation of the concept. The heat transfer characteristics of a typical cell should be determined. All parameters such as current density and voltage should be correlated as a function of subsystem variables.

Should more sophistication in the math models be desired, an example of where improvements could be made is in the technique for establishing the water transfer rate to the exit streams. Currently the rate is established by fixed input data for relative humidity in the exit streams. A more realistic model could be developed based on the actual transport phenomena occurring. The math model for predicting water transport rates in the component for humidifying process gas prior to entering the cells also is an example where improvement might be warranted.

### 3.4 Hydrogen Depolarized Cell

The mathematical model for this subroutine was prepared by Hamilton Standard in conjunction with subsystems development studies for the SSP program. As such the routine should provide a good representation of the subsystem.

### 3.5 Solid Electrolyte Cell

A good comparison between subsystem results with test data was obtained for this subsystem. This was possible to a great extent because of the advanced state of development of the concept. Good documentation of subsystem test results also was available (Reference 18).

It should be noted that the mathematical model for the solid electrolyte cells is somewhat empirical in nature. That is, the model relies heavily on the experimental data. Overall current efficiency,  $H_2$  or CO current efficiency, cell voltage (or voltage efficiency) are a few of the parameters which are based on experimental results. While theoretical relationships could be developed, they would not be as accurate as the empirical data. In order to insure accurate computer results over a wide range of operating conditions, additional laboratory testing is required to determine correlations for these critical parameters as a function of operating variables.

A more detailed mathematical model for the carbon deposition reactor could be developed by treating the reactor as a classical tubular reactor. Additional experimentation would be required to determine the effects of reactor geometry and catalyzing effects on the kinetics of the reaction. In particular, the catalyzing effects of the reactor steel wall and water vapor in the inlet stream would have to be incorporated into the rate equations. Alternatively correlations could be developed for CO and  $H_2$  conversion efficiencies as a function of operating variables.

### 3.6 Liquid Absorption

The mathematical models prepared for the simulation of this concept should be adequate for gross system analysis. More complex models are not warranted at this time since the concept is only in a conceptual stage of development. Many problems remain to be solved in designing zero-g hardware.

When the design concept becomes better defined, there are several areas where improvements could be made in the mathematical models. For the liquid contractor, a subroutine could be prepared with a multiple number of bed elements. Transient macroscopic mass and energy balances could be set-up taking into account mass transfer resistances in both the liquid and gas phases.

Another subroutine which might warrant future development would be an air/liquid separator routine. The subroutine would be modeled after zero-g separator devices currently in the state of development. The separation achieved would be predicted from constituent equilibrium relationships and efficiency factors.

The subroutine for the separation of  $CO_2$  from the liquid phase has been modeled as an equilibrium or flash vaporization process. When the design of this device is better defined, the subroutine would be modified to better reflect the operating characteristics of the device.

It is suggested that system analysis studies be performed leading to the development of a space hardware prototype for this subsystem. Improvements to the existing subroutines could be made concurrently with the prototype development.

### 3.7 Electrodialysis Cells

The subroutine prepared for this concept should provide an adequate simulation of the "E" stack cell configuration described in reference 21. For this configuration a considerable amount of oxygen is generated along with the removal of  $\text{CO}_2$ . One possible improvement in the routine might be to provide an option for simulating the "F" configuration, which minimizes  $\text{O}_2$  production.

The subroutine prepared relies on experimental data for stack voltage, power and current efficiencies. It is suggested that correlations be developed for these parameters as a function of operating variables.

A more sophisticated method for determining the amount of water lost by electro-endosmosis probably is warranted. The current method is based on fixed input values for the humidities in the exit streams. A model based on the physical chemistry of the actual phenomena could be developed and incorporated into the subroutine.

### 3.8 Molten Carbonate Cells

The subroutine prepared should allow good simulation of molten carbonate cells in which the process air has been pre-dried to prevent water vapor electrolysis and subsequent adverse side reactions. Should future subsystem studies indicate the advisability of developing a cell for combined  $\text{CO}_2$  removal and  $\text{H}_2$  electrolysis, additional logic would have to be incorporated to simulate the side reactions.

The current subroutine relies on experimental values for power efficiency. Current efficiency is assumed to be 100%. Correlations should be developed for these parameters over a range of operating conditions. While current efficiency should approach 100% for the expected operating conditions, excessive current densities will cause degraded performance.

### 3.9 Membrane Diffusion

The mathematical model prepared for the diffusion separator should allow a good simulation of this concept. In addition, the subroutine can be used to simulate similar diffusion processes in other subsystems.

The most important parameters, which must be accurately defined, are the permeabilities of the diffusing species. Correlations for permeabilities as a function of system variables should be determined by additional laboratory testing.

### 3.10 Mechanical Freezeout

No new component subroutines were prepared in order to simulate this concept. A modified version of the heat exchanger subroutine was used to simulate the precipitator and sublimator. The partial pressure of  $\text{CO}_2$  leaving the precipitator is predicted from the equilibrium sublimation curve for  $\text{CO}_2$  and Dalton's law. Mass transfer rates are not considered. The rate of  $\text{CO}_2$  leaving the sublimator is assumed to equal the rate of precipitation. The heat exchanger subroutine calculates the required outlet temperature for the heating fluid necessary to provide the heat of sublimation.

The technique for simulating the precipitation process should provide an adequate simulation. The transient simulation of this process could be improved by preparing a multi-element model with the rate of mass transfer calculated from an overall mass transfer coefficient and the difference between the gas phase partial pressure and the  $\text{CO}_2$  equilibrium partial pressure.

The improvements suggested above are even more important for an adequate transient simulation of the sublimator. In order to develop such a model, the design geometry of the precipitator/sublimators must be fully defined. In addition, experimental testing would be required to determine a correlation for mass transfer coefficients as a function of system parameters.

## REFERENCES

1. Tepper, F.; Vancheri, F.; Samuel, W. and Vdavcak: Development of a Regenerable Carbon Dioxide Removal System. NASA CR-66571 (MSA Research Corporation) Jan 1968.
2. MSA Research Corporation: Development of System Design Information for Carbon Dioxide Using an Amine Type Sorber. NASA CR-11849, June 1971.
3. Brose, H. F. and Martin, R. B. Performance of a Solid Amine Carbon Dioxide Concentrator During a 90-Day Manned Test. NASA SP-261, p. 131-144, November 1970.
4. Glueckert, A. J., Nuccio, P. P., and Zeff, J. D.: "GAT-O-SORB - A Regenerable Sorbent for Carbon Dioxide Control." SAE Paper No. 670844, Aeronautic and Space Engineering and Manufacturing Meeting, Los Angeles, California October 1967 (General American Transportation Corp.).
5. Glueckert, A. J., Nuccio, P. P., and Zeff, J. D.: GATC Report MRD 1230-4050, Final Technical Report for a Prototype Regenerable Carbon Dioxide Removal System, Contract No. NAS1-2915, MRD Division General American Transportation Corporation, August 1964.
6. Huebscher, R. G. and Babinsky, A. D.: "Electrochemical Concentration and Separation of Carbon Dioxide for Advanced Life Support Systems - Carbonation Cell System". SAE Paper No. 690650. National Aeronautic and Space Engineering and Manufacturing Meeting, Los Angeles, California. October 1969.
7. Wynveen, R. A. and Quattrone, P. D.: "Electrochemical Carbon Dioxide Concentrating System". ASME Paper No. 71-AV-21, July 1971.
8. Kiraly, R. J., Babinsky, A. D., and Quattrone, P. D.: "On-Board Oxygen Generating System". SAE Paper No. 680716, SAE Meeting, Los Angeles (Oct. 1968).
9. Quattrone, P. D., Babinsky, A. D., and Wynveen, R. A.: "Carbon Dioxide Control and Oxygen Generation". ASME Paper No. 70-AV/SPT-8, ASME Meeting, Los Angeles (June 1970).
10. Huebscher, R. G., and Babinsky, A. P., "Aircrew Oxygen System Development, Carbon Dioxide Concentrator Subsystems Report," NASA CR-73397 (1970).

11. Sribnik, F., Dean, W. C., Aylward, J.: "Hydrogen Depolarized Cell/Water Vapor Electrolysis Cell".  $\text{CO}_2$  Collection Subsystem Preliminary Design Package, SSP Document No. A35 (HSD Report).
12. Brose, H. F. "Hydrogen Depolarized Cell for a  $\text{CO}_2$  Concentrator," ASME Paper No. 71-Av-37. SAE/ASME/AIAA. Life Support and Environmental Control Conference (July 1971), San Francisco.
13. Chandler, H. W.; Carbon Dioxide Reduction System. Isomet Corp., Contract No. AF33(657)-8066, Report No. AMRL-TDR-64-2, May 1965.
14. Chandler, H. W. and Howell, L. J., A Solid Electrolyte Carbon Dioxide Reduction System. Aerospace Medical Research Laboratories Report, AMRL-TR-67-209. January 1968.
15. Trade-off Study and Conceptual Design of Regenerative Advanced Integrated Life Support Systems, Hamilton Standard Division of United Aircraft Corp., Report No. NASA CR-1458, January 1970.
16. Weissbart, J.; Smart, W. H.; Wydeven, T.: "Design and Performance of a Solid Electrolyte Oxygen Generator Test Module". ASME Paper No. 71-AV-8. SAE/ASME/AIAA Life Support Meeting, San Francisco, California, April, 1971.
17. Elekan, L., Morris, J. P., Wu, C. K., Saunders, C. G.: "180-Day Life Test of Solid Electrolyte System for Oxygen Regeneration", ASME Paper No. 71-AV-32, ibid.
18. Elikan, L. and Morris, J. P.; "Development of a Solid Electrolyte System for Oxygen Regeneration". Contract NAS1-8996, Westinghouse Electric Corp., Pittsburg, Pa.
19. Perry, R. H., "Chemical Engineers Handbook", 4th Edition, p. 14-11, McGraw-Hill, New York, 1960.
20. Ionics, Inc.: "Carbon Dioxide Removal and Water Electrolysis Subsystems". Sept. 1963 (Proposal document to Douglas describing system operation and performance).
21. Brown, D. L.: "Investigation of an Electrochemical Device for Carbon Dioxide Absorption and Oxygen Generation". ASD TDR 63-441, May 1963 (Ionics)
22. Stein, P. J.: Research and Development Program for a Combined Carbon Dioxide Removal and Reduction System. Hamilton Standard Division, Contract No. NAS1-4154, Final Report - Phase I, October 1965.

23. Arnoldi, W. E.: "An Electrolytic Process for Carbon Dioxide Separation and Oxygen Reclamation". Atmosphere in Space Cabins and Closed Environments, Meredith Publishing Co., 1966, pp. 76-103.
24. Newlander, C. K., Martin, F. J., "Development of a Permselective Membrane System for Continuous Carbon Dioxide Control", AMRL-TR-70-44, October 1970.
25. Maulbetsch, J. S., "An Experimental Investigation and System Design for Humidity and Carbon Dioxide Level Control Using Thermal Radiation", AMRL-TR-68-174 (April 1969). Dynatech.
26. Schaffer, A: "Analytical Methods for Space Vehicle Atmospheric Control Processes. SS-572-R (1961). AiResearch Manufacturing Company.
27. Dulock, V. A.: "Preliminary Heat Rejection Rates and Thermal Radiator Area Requirements for a Freeze-Out Life Support System". TRW Systems, Houston Operations in-house report (November 1970).
28. Bonneville, J. M.: "A Study of Water and Carbon Dioxide Precipitation Techniques Using Thermal Radiation Principles". AMRL-TR-66-118. (Aug. 1966) Dynatech.

APPENDIX A

G-189A ETC/LS SYSTEM ANALYSIS PROGRAM DESCRIPTION

## PROGRAM DESCRIPTION

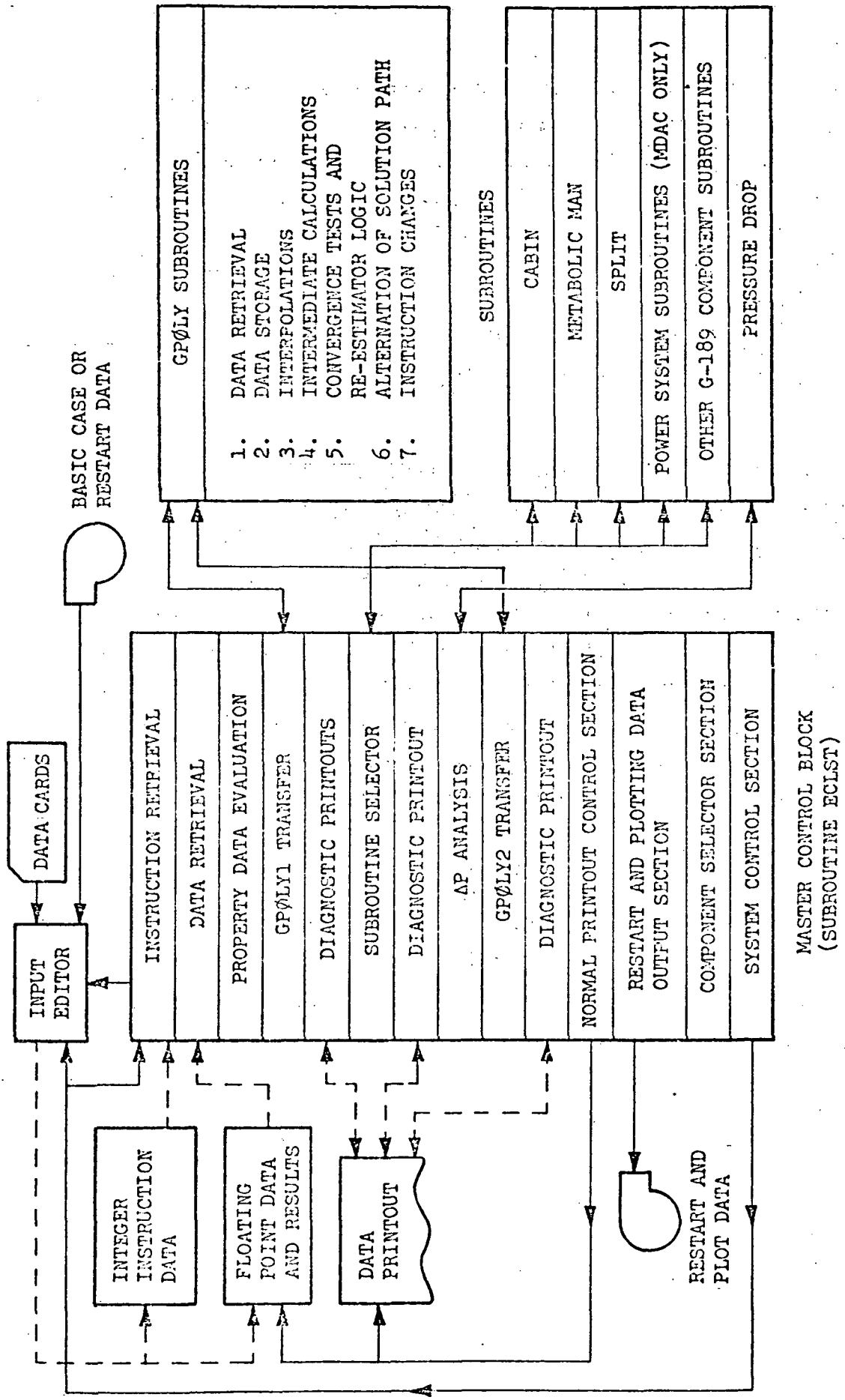
The G-189A ETC/LS System Analysis Program provides a basic simulation tool for studying the steady state and transient performance of an ETC/LSS. An ETC/LS system is simulated with the program by describing the equipment in terms of individual "components" which are connected by gaseous or liquid flow streams. Each particular type of component is simulated by an individual component subroutine contained within the G-189A program. A component corresponds to all or part of a physical part; such as a tee, heat exchanger, electronic coldplate, etc.; or to a complete subsystem or process; such as  $\text{CO}_2$  concentration,  $\text{O}_2$  recovery, etc. The individual components of the simulation are arbitrarily assigned successive integer numbers which are used to define the component flow stream interconnections and to specify the computational sequence of the individual components. The interconnection and sequence data are specified by the user and may be easily changed. The computational sequence generally follows a path corresponding to the ETC/LS system flow stream paths.

The G-189A component subroutines perform heat transfer, chemical reaction, and mass and energy balances for both steady state and transient operating conditions. System pressure drop versus fan or pump pressure rise balances can also be performed if desired. Examples of energy balances are: (1) the summation of cabin gas heat rejection rates from individual sources within the cabin balanced with the total heat load imposed on the cabin heat exchanger and (2) the summation of individual coolant loop heat loads balanced with the heat rejected by the space radiators. Examples of mass balances include the balancing of water vapor and  $\text{CO}_2$  generation rates from the crewmen against the cabin leakage rates, gas supply rates, and system equipment removal rates.

The G-189A program is essentially comprised of seven sections: (1) a main subroutine or Master Control Block (MCB); (2) an Input Editor; (3) two user coded subroutines, GP $\varnothing$ LY1 and GP $\varnothing$ LY2, for implementing additional computational logic; (4) a set of ETC/LSS component subroutines; (5) a pressure drop analysis subroutine; (6) a set of utility subroutines; and (7) a SD-4060 plotting package.

Figure A-1 presents a block diagram of the G-189A program logic. The program operations and their sequence are determined by the Master Control Block (MCB), also known as subroutine ECLST. The operations performed by the MCB are indicated in the center block of Figure A-1. The G-189A program sequence of operations, as shown in Figure A-1, is described below:

1. At the start of execution the MCB initiates a call to the Input Editor to process a set of simulation data.
2. The Input Editor processes simulation data taken from cards, tape, and/or disk; allocates the data storage; dynamically loads the integer and floating point data into a large single array (K or V array); and prints the edited card images.
3. The MCB prints out the solution path and component initial value data as input. Component calculations are begun starting with the first component in the specified solution path.
4. The component integer instruction data are retrieved and unpacked and floating point data are retrieved and stored in smaller working arrays (A, B, and R arrays) for use during component solution.
5. Thermophysical property data (specific heat, molecular weight, thermal conductivity, and viscosity) for the component source flow streams are evaluated.
6. A transfer to the user coded subroutine GPØLY1 is made to allow data modifications or logic changes to be incorporated prior to component solution. Upon return an optional diagnostic printout of the working arrays (A, B, and R array) is available.
7. A transfer to the proper component subroutine for component solution is made. Following component solution a transfer to the user coded subroutine GPØLY2 is made to allow data modifications or logic changes after component solution. Upon return from GPØLY2 an optional printout of the working arrays is available.
8. If a pressure drop model is being executed, a transfer to the pressure drop analysis subroutine is made. Upon return an optional printout of the working arrays is available.



9. At the end of a component's solution and pressure drop analysis the calculated component data are stored into the large data storage array (K and V array) and, if specified, the component results stored in the K and V array are printed. If the current component is the last one in the system solution path and the end of steady state or transient has occurred, a complete printout of all components' integer and floating point data is made.
10. Restart and/or plotting data are output to tape or disk; if specified, at the end of steady state calculations and at the end of transient system passes.
11. The completion of steady state, pressure drop/fan or pump balance, and transient calculations are determined by the MCB. If the calculations are not finished the next component to be solved is selected and component solution is re-initiated (Items 4-11). (Pressure drop/fan or pump balance iterations during transient allow only changes in the mass flow calculations to occur within the component subroutines - thermal, chemical reaction, and energy calculations are not made and system simulation time is held constant.) If the current case has been completed any plot data stored during the case are processed and a transfer is made to the Input Editor to process the next set of case data. Iterations continue through items 1-11 until all case data have been processed or until an unrecoverable program error occurs.

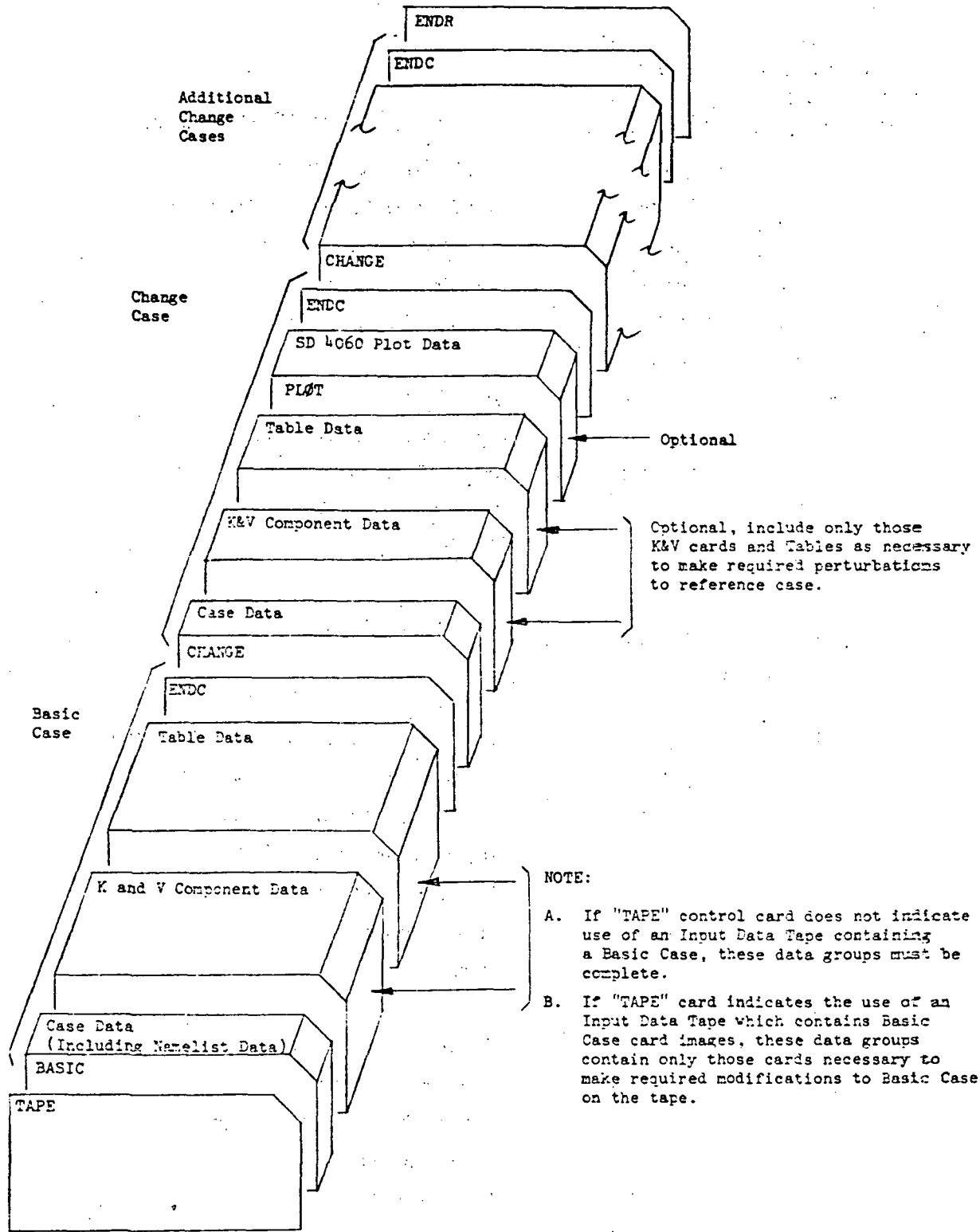


FIGURE A-2

**COMPONENT SUBROUTINE LIST**

<u>Component Subroutine Number</u>	<u>Subroutine Fortran Name</u>	<u>Subroutine Description</u>
1	CABIN	Cabin or Compartment
2	SUITS	Simplified Crewman Simulation
3	CMAN	2-Node Metabolic Man
4	ANYHX	Heat Exchanger
5	ELCELL	Electrolysis Cell
6	GASMIX	Gas Mix
7	LIQMIX	Liquid Mix
8	ELCØØL	Electronic Coldplate
9	RDIATR	Space Radiator or Solar Absorber
10	SPLIT	Generalized Split
11	ADSØRB	Adsorption Bed
12		
13	CATBRN	Catalytic Burner
14		
15	SERVØ	Automatic Controller
16	DUCT	Gas Duct (Heat Loss to Surroundings)
17	PIPE	Liquid Loop Pipe (Transport Lag & Heat Loss)
18	ELPTRT	Electrolytic Pretreatment
19	VAPCØM	Vapor Compression/Distillation
20	AIRVAP	Air Evaporation
21	BØSCH	Bosch Reactor
22	PUMP	Pump
23	FAN	Fan
24	CARCL1	Carbonation Cell - 1st Stage
25	CARCL2	Carbonation Cell - 2nd Stage
26	HUMIDT	Humidifier/Dehumidifier
27*	SMGEN	Steam Generator
28*	VACPMP	Vacuum Pump
29	FLØMET	Averaging and Totalizing Flowmeter
30	TANKG	Accumulator Tank

\*New subroutine prepared for this contract

COMPONENT SUBROUTINE LIST (continued)

<u>Component Subroutine Number</u>	<u>Subroutine Fortran Name</u>	<u>Subroutine Description</u>
31	SABAT	Sabatier Reactor
32	H2DP $\emptyset$ L	Hydrogen Depolarized Cell
33	HTSINK	Heat Sink/Thermal Capacitor
34	HTCAPC	Heat Sink/Thermal Capacitor
35	VERTHM	Wax Element Control Valve
36*	COS $\emptyset$ RP	Two Constituent Sorption Bed
37	THERML	Thermal Analyzer
38		
39		
40		
41	AGZNPB	Silver/Zinc Primary Battery
42	DCDCRC	DC/DC Regulated Converter
43	DCL $\emptyset$ AD	DC Electrical Load Profiel
44	EJN $\emptyset$ DE	Electrical Junction (Ground)
45	SPN $\emptyset$ DE	Electrical Bus
46	GEL $\emptyset$ AD	Generalized Electrical Load (Motor, Relays, etc.)
47	FCREAC	Fuel Cell Cryogenic Reactant Rate Component
48	FCELT	Fuel Cell Electrical Component
49	ALTC $\emptyset$ M	Dummy or Alternate Component
50*	CARDP	Carbon Deposition Reactor
51*	S $\emptyset$ LEL	Solid Electrolte Cells
52*	LIQC $\emptyset$ N	Liquid Contactor
53*	ELDIAL	CO <sub>2</sub> Electrodialysis
54*	MLCARB	Molten Carbonate Cell
55*	MEM $\emptyset$ D	Membrane Module
56*	LQFLSH	Liquid Flash Vaporizer

\* New subroutine prepared for this contract.

**MCDONNELL DOUGLAS ASTRONAUTICS COMPANY**

5301 Bolsa Avenue, Huntington Beach, California 92647 (714) 897-0311